# Predicting Local Seismic Damage of Reinforced Concrete Framed Buildings considering the Horizontal Seismic Component

**M.A. YOUSSEF**[1]
**M.A. ELFEKI**[2]

[1] Western University, Department of Civil and Environmental Engineering, London, ON N6A 5B9, Canada
[2]Alexandria University, Department of Civil Engineering, Cairo, Egypt

This paper provides a simplified method to define local seismic damage for reinforced concrete frames considering the horizontal seismic component. The proposed method utilizes static pushover analysis to evaluate the maximum and residual inter-storey drift limits for each storey. These limits are predicted for five frames and compared to experimental and analytical results by other researchers. Further validation of the method is achieved by conducting incremental dynamic analyses for a concrete frame using five earthquakes. Results have also provided an assessment of the use of residual and maximum inter-storey drifts to define collapse.

*Keywords*: Seismic, Reinforced Concrete, Moment Frame, Seismic Damage, Residual Drift, Maximum Drift.

## 1- Introduction

During the last two decades, evaluating the seismic performance of Reinforced Concrete (RC) structures received significant attention by the research community. Several criteria were proposed to judge on the severity of seismic damage. These criteria include defining values for strains or curvatures to predict local damage and values for Maximum Inter-storey Drift (MID) to predict global damage. A RC building is expected to sustain severe global and local damage if the Inter-storey Drift (ID) of any floor exceeds a pre-defined MID. Researchers proposed different values for MID at collapse including 2% (Sozen, 1981), 2.5% (SEAOC, 1995), 3% (Broderick and Elnashai, 1994; Kappos 1997), 4% (FEMA 273, 1997), 5.6% (Ghobarah et al., 1998), and 6% (Roufaiel and Meyer, 1983). Dymiotis (2000) established statistical distribution of the MID at collapse using existing shake table results of small-scale bare frames. This distribution, Fig. 1, shows that MID varies from about 3% to about 16%. MID is also used to define other levels of performance. For example, the life safety level is reached at MID of 2% (FEMA 273, 1997).

The observed large variation in the values of MID at collapse can be attributed to design assumptions, variation of the drift limit of columns with the applied axial force, sensitivity of the seismic performance to magnitude, Peak Ground Acceleration (PGA), and frequency content of the earthquake, and effects of higher modes of vibration.

The permanent displacement experienced by a structure following a seismic event can be used to judge on its residual capacity (Bazzurro et al., 2004). Toussi and Yao (1982) and Stephens and Yao (1987) defined four levels of structural damage using Residual ID (RID). FEMA 273 (1997) introduced the use of RID to allow onsite evaluation of the safety of seismically damaged buildings. Values of 3% and 1% are specified for collapse and life safety limits.

During the past five years, research studies were conducted to evaluate the parameters affecting the RID and its efficiency as compared to MID. The amplitude of the RID was found to be affected

by the ratio of post-yield stiffness to initial elastic stiffness (MacRae and Kawashima, 1997) and the hysteretic behaviour (Christopoulos et al., 2003; Ruiz-Garcia and Miranda, 2006). Medina and Krawinkler (2003) noted that the distribution of the residual drift of regular one-bay RC frames along the height is similar to the distribution of the MID. Disadvantages of RID as compared to MID include: (1) higher influence of record to record variability (Ruiz-Garcia and Miranda, 2006) and (2) non-uniform and large dispersion of residual drifts along the height (Medina and Krawinkler, 2003).

This paper presents the development and validation of a simplified method that predicts the collapse limit and identifies the locations of local seismic damage.

## 2- Proposed method

The proposed method is based on defining the ID and RID at collapse for each storey. Pushover analysis is employed to calculate these values for each storey individually. The columns of the considered storey are assumed to be fixed at their lower ends (ignoring the lower stories). Gravity loads are then applied to the studied storey and the stories above it to account for the variation of the column axial loads and the P-Δ effect. Fig. 2 shows application of the proposed method to the fourth storey of a six-storey building. A displacement controlled pushover analysis is applied at the considered storey to define the ID at collapse. Unloading from the collapse point allows defining the RID at collapse. Failure is assumed to be reached when the core concrete of all storey columns reach its crushing strain. ID and RID at collapse are then magnified to account for the reduction of the lateral stiffness due to the rotation of the lower column ends.

Calculations of the magnification factors are based on the approximate method developed by Muto (1974) and modified by Paulay and Priestley (2009). The method is modified to account for the

variation of beam stiffness rom a floor to another. For prismatic elastic columns that are fully restrained against rotation, Fig. 3a, the ID is equal to Δ and corresponds to a shear force $V_f$.

$$V_f = \frac{12E_cI_c}{h^3}\Delta \quad (1)$$

where $E_c$ is the modulus of elasticity for columns, h is the column height, and $I_c$ is the moment of inertia of the column.

As columns are partially restrained by the beams above and below the studied storey, Fig. 3b, the shear force $V_i$ can be calculated using Eq. 2.

$$V_i = \alpha \, . \, V_f = \alpha \, \frac{12E_cI_c}{h^3}\Delta \quad (2)$$

Where $\alpha$ is a reduction factor for the lateral stiffness to account for the rotations at the column ends.

It is proposed to calculate $\alpha$ using the following assumptions (Fig. 4): (1) joint rotations are equal for any two successive stories (θ), (2) the stiffness of each beam is equally utilized by the columns above and below a specific floor (beams are split into hypothetical halves, each half possesses 50% of the stiffness of the original beam), and (3) Contra-flexure points are assumed to be at the mid-span of each beam and mid-height of each column. The stiffness is presented in the figure by the ratio K where K = I/L,

Fig. 5 shows an isolated column and the beams connecting to it. The pinned ends of beams represent the points of contra-flexure. When a relative drift Δ is imposed between the column ends, the resulting column shear $V_i$ can be calculated by following these steps:

(1) The fixed end moment induced by this displacement is calculated using Eq. 3.

$$M_F = \frac{V_f h}{2} = \frac{1}{2}h \cdot \frac{12E_cI_c}{h^3} \cdot \Delta \quad (3)$$

(2) The flexural stiffness of the top beams and the column are $3E_bK_1$, $3E_bK_2$ and $6E_cK_c$. The moment distribution factor $d_{ct}$ can thus be calculated using Eq. 4.

$$d_{ct} = \frac{6E_cK_c}{3E_c(n_bK_1 + n_bK_2 + 2K_c)} = \frac{2}{\bar{K}_t + 2} \tag{4}$$

Where $E_b$ is the modulus of elasticity of the beams, $n_b = E_b/E_c$, and $\bar{K}_t$ is given by Eq. 5.

$$\bar{K}_t = \frac{n_b(K_1 + K_2)}{K_c} \tag{5}$$

(3) Using the principle of moment distribution, the final moment acting at the top of the column is given by Eq. 6.

$$M_{ct} = \frac{1}{2}h \cdot \frac{12E_cI_c}{h^3} \cdot \frac{\bar{K}_t}{\bar{K}_t + 2} \cdot \Delta \tag{6}$$

Similar equation can be derived for the moment at the bottom end of the column

$$M_{cb} = \frac{1}{2}h \cdot \frac{12E_cI_c}{h^3} \cdot \frac{\bar{K}_b}{\bar{K}_b + 2} \cdot \Delta \tag{7}$$

Where:

$$\bar{K}_b = \frac{n_b(K_3 + K_4)}{K_c} \tag{8}$$

(4) The column shear resulting from the relative drift is given by Eq. 9

$$V_i = \frac{M_{ct} + M_{cb}}{h} = \alpha . \frac{12E_cI_c}{h^3} \cdot \Delta \tag{9}$$

Where $\alpha$ can be calculated using eq. 10

$$\alpha = \frac{1}{2}\left[\frac{1}{\frac{2K_c}{K_1 + K_2} + 1} + \frac{1}{\frac{2K_c}{K_3 + K_4} + 1}\right] \tag{10}$$

Equations 3 and 9 indicates that the displacement for a partially restrained column is equal to that for a fully restrained column multiplied by a drift magnification factor m, m=1/ α. An average value, $m_{av}$, for each storey is proposed to be calculated using Eq. 11.

$$m_{av} = \frac{\sum \text{stiffnesses of storey columns assuming fully fixed conditition}}{\sum \text{stiffnesses of storey columns assuming partially fixed condition}} \quad (11)$$

**3- Local Failure Criteria**

Local yielding of elements is assumed to occur when the tensile strain in the longitudinal reinforcement reaches its yield strain ($\varepsilon_y$= 0.002). A number of criteria were suggested by different researchers to define local failure of concrete members. These criteria include defining a value for ultimate curvature or crushing strain (Mwafy and Elnashai 2001). The crushing strain is expected to depend on the type of concrete, the level of confinement, and the level of axial force. The crushing strain was found to be varying from 0.0025 to 0.006 for unconfined concrete (MacGregor and Wight, 2005) and from 0.015 to 0.05 for confined concrete (Paulay and Priestley 1992).

A typical concrete stress-strain curve including unloading and reloading branches is shown in Fig. 6 (Mander et al., 1988). For the proposed method which relies on pushover analysis, crushing was assumed to occur when the confined concrete strain reaches the lower bound value of 0.015. For dynamic analysis and due the loading and reloading paths, reaching this lower bound value of 0.015 at a given instant will not represent the crushing state. Instead crushing was defined to occur when the stirrups reach their fracture strength as proposed by Pauley and Priestley (1992), and given by Eq. 12.

$$\varepsilon_{cu(\text{confined concrete})} = \varepsilon_{cu(\text{unconfined concrete})} + \frac{1.4\rho_s f_y \varepsilon_{sm}}{k_h f_c'} \quad (12)$$

where $\rho_s$ is the ratio of the volume of transverse reinforcement (RFT) to the volume of concrete

core measured to outside of the transverse RFT, $f_y$ is the steel yielding stress, $\varepsilon_{sm}$ is the steel strain at maximum tensile stress and $K_h$ is the confinement factor.

**4- Computer Program**

Due to the complexity of calculating the seismic response of RC structures, a powerful finite element tool is needed. The finite element program ZEUS-NL (Elnashai et al., 2002) is utilized in this study. The program is capable of representing spread of inelasticity within the member length using the fibre analysis approach. ZEUS-NL can be used to predict response of RC frames under static or dynamic loading and it takes into account both geometric and material nonlinearity.

The program was used by Jeong and Elnashai (2005) to simulate a full scale dynamic test of an irregular RC three storey building. The program was found to be capable of predicting the drifts including residual drifts with high accuracy. To further validate the accuracy of ZEUS-NL in estimating the peak and residual drifts defining failure, the experimental measurements reported by Abrams (1987) for lateral behaviour of cantilever RC columns under constant and variable axial loads were utilized. Fig. 7 shows a comparison between the experimental and analytical moment rotation relationships. It can be noticed from the figures that the difference between the predicted and measured rotations including residual rotations in both cases is less than 10%. The single cantilever column tested by Sakai and Mahin (2004) is considered to further validate ZEUS-NL. The column was subjected to two of the components of Los Gatos earthquake, Loma Prieta 1989, scaled to different intensities (Sakai and Mahin, 2005). The column was modeled and analyzed using ZEUS-NL. The dynamic analysis was conducted using the two components of Los Gatos record scaled to 70% and 100%. Table 1 shows comparison between the experimental results and the results of the dynamic analysis at both scales. The maximum and residual drifts are predicted with suitable accuracy (maximum error of 20%).

## 5- Validation of the proposed method

In this section, predictions of the proposed method are compared to the analytical or experimental results by others (Ghobarah et al., 1999; Lu, 2002; Moehle et al., 2005, and Haselton and Deierlein, 2008). The buildings selected by these researchers are reanalyzed using the proposed method to predict the ID at collapse and to identify the floor sustaining the most damage. The number of stories and bays for each of the buildings are summarized in table 2. Rigid link members were added at the beam column joints, Fig. 8, as the buildings were designed according to new codes requirements and joint shear deformations were expected to be minimal. The reported MID at collapse and the floor sustaining the most damage are summarized in table 2. The two three-storey RC frame office buildings studied by Ghobarah et al. (1999) represent a nonductile and a ductile moment resisting frames. The buildings were subjected to four different earthquake records scaled to different intensities. The proposed method is applied to estimate the MID at collapse and the location of the critical storey. Concrete models accounted for the differences between the confinement ratio in the ductile and the nonductile frames. Bond slip and joint shear deformations were minimal in both frames (Ghobarah et al., 1999). Table 2 shows good agreement between the collapse drift limits estimated by the proposed method and by Ghobarah et al. (1999). Also both results show that the first storey experiences the highest damage.

The six-storey building tested by Lu (2002) has a vertical irregularity as all of its floors have 3 bays except the 1$^{st}$ floor which has 2 bays. The building is designed according to the requirements of Eurocode 8 (1994) and is tested using the N-S component of 1940 El Centro earthquake record scaled to PGA of 0.10g, 0.30g, 0.60g, and 0.90g. It is observed from the experimental work that the building remained perfectly stable at 0.6g with very minor cracks (2.4% MID) and collapsed due to soft first storey mechanism at 0.9g (6% MID). It is also observed that the fifth storey columns

suffered some damage at an ID of 4%. Fig. 9 shows the collapse limits as predicted by the proposed method compared to experimentally measured IDs. It is clear from the figure that the ID at the first storey exceeds the collapse limit, and thus failure occurred due to a soft first storey. To judge on the ability of the proposed method in evaluating the damage state of the $5^{th}$ storey at 4% ID, a pushover analysis for the fifth storey is conducted using the same procedure shown in Fig 2. The ID magnification factor given by Eq. 11 is 1.578, and thus pushover analysis is applied to an ID of 2.53%. At this level of ID, strain in the tensile reinforcing bars of the columns reached the yielding value explaining the severe cracking. Also, the unconfined concrete of the columns reached its crushing strain and expected to spall off.

The three storey building tested by Moehle et al. (2005) using a shake table at the University of California, Berkeley has four columns; two of them have nonductile detailing while the other two columns are detailed according to the ACI 318-2002 recommendations. The building was subjected to seven ground motion time histories recorded during the 1994 Northridge earthquake. The building is analyzed using the proposed method to predict the MID at collapse. Different concrete models are used to represent the reinforcement details of different members. Joints were reinforced according to the new seismic provisions (Moehle et al., 2005), and thus joint shear deformations are expected to be minimal. Zero length shear springs are added to the ends of the non ductile columns to model the hysteretic shear–axial interaction (Lee et al., 2005). As shown in table 2, there is good agreement between the results obtained by Moehle et al. (2005) and those obtained by the proposed method.

Using 40 records, Haselton et al. (2008) conducted an incremental dynamic analysis on a four storey building to assess the seismic safety of modern RC moment-resisting frame buildings. It can be noted that the values of MID at collapse from this study ranged between 4.00 and 12.00% depending on the input ground motion and the storey experiencing the most damage. The proposed

method provides a single value for Failure ID (FID) for each storey. The FID limits for the first and second stories are 4.00% and 9.00%, respectively. The FID limit of the 1st storey can successfully explain the lower bound of the observed MIDs. The contribution of the second storey to the failure mechanism for some of the records resulted in a higher FID that can be explained by the second storey FID limit predicted by the proposed method.

## 6- Case Study

In this section, a symmetric six-storey RC office building is considered to further validate the proposed method and to provide a comparison between the effectiveness of using either ID or RID to estimate seismic damage in a specific floor. The selected dimensions and layout of the building are shown in Fig. 10a. The building is selected to be in a highly seismic region such as California. It is designed according to the regulations of the International Building Code (IBC, 2006) and the ACI requirements (ACI 318, 2005) for both gravity and seismic loads. The concrete unconfined compressive strength is 28 MPa and the reinforcing steel yield strength is 400 MPa. The dead loads include the weight of the structural elements and the masonry walls. The live load is assumed equal to 4.8 KN/m$^2$, which is a typical value for office buildings. The seismic loads are resisted by special moment frames as defined in ACI 318 (2005). Section dimensions and reinforcement details for a typical moment frame are given in Fig. 10b. Eigen value analysis is performed to determine the natural periods of the structure. The fundamental horizontal period of vibration is found equal to 0.501 sec. The first four mode shapes are shown in Fig. 11.

As the structure is symmetric, a 2D model is used. Beams and columns are modeled using cubic elasto-plastic elements. Beam elements are divided into six elements to match the distribution of longitudinal and transverse reinforcements. Column elements are divided into three elements; two short elements at the ends and a middle element. Such a modeling technique allows monitoring

local damage at the ends of each element. The frame beams are modeled as T-sections assuming an effective flange width equal to the beam width plus 14% of the clear beam span (Jeong et al., 2005). The beam-column connections are modeled using rigid elements as shown in Fig. 8 for an interior joint and Fig. 12 for an edge joint.

The collapse limits for the six-storey building are estimated in terms of ID and RID using the developed method. Drift magnification factors are calculated for each storey using Eq. 11 assuming gross moment of inertia for all elements. This assumption is reasonable for high values of drift as the damage level for both beams and columns is expected to be relatively similar. The calculated magnification factors are summarized in table 3. The FID and the corresponding RID are summarized in Fig. 13. The first storey has the lowest collapse limit (3.064% FID ratio and 2.530% RID ratio). This storey is expected to sustain high local damage during dynamic analyses. The third storey seems to be a critical storey as well.

### 6.1- Static Pushover Analysis

Inelastic pushover analysis for the full frame is performed. The vertical distribution of the lateral load is taken similar to the distribution used in the design. A force controlled pushover is employed up to the maximum base shear. The analysis proceeds by using displacement control up to failure followed by unloading of the applied forces.

Fig. 14a shows the pushover curve for the six-storey building. The building lateral capacity is about 1.8 times the design base shear. At collapse, the predicted maximum roof drift and the residual roof drift are equal to 2.2% and 1.6%, respectively. The expected damage in the six-storey frame at collapse is shown in Fig. 14b.

Figs. 15a and 15b show comparison between the distribution of the IDs and RIDs at collapse as obtained using the proposed method and pushover analysis. It can be observed from the figures that ID and RID of the first storey are equal to 3.070% and 2.530%, respectively. These values are higher than the predicted FID and RID limits, which explains the observed crushing at the lower ends of four of the first storey columns, Fig. 14b. Also figure 15 shows that the third storey is having high values of ID and RID if compared to the predicted collapse limits. Fig. 14b shows that one of the third storey columns has reached the crushing strain at its top end. Although the second storey experienced the highest ID and RID, none of its columns reached the crushing strain. The calculated limits clearly show that this floor is not a critical one. Such an observation clearly shows the need for using a collapse limit for each storey instead of using a single value of MID or Maximum RID. Based on the results of the pushover analysis, using either the FID or RID of the proposed method results in accurate prediction of the critical storey.

**6.2- Dynamic Analysis**

Five earthquake records are selected to examine the behaviour of the designed RC building at collapse. These records cover a wide range of ground motion frequencies represented by the ratio between the PGA and the peak ground velocity (A/v ratio). The characteristics of the chosen records are presented in table 4. Available methods to scale the ground motion records include scaling of the PGA, the Peak Ground Velocity, and the 5% damped spectral acceleration at the structure's first period [Sa (T1, 5%)]. Scaling based on Sa (T1, 5%) was found to be the most reliable method (Shome and Cornell, 1999; Vamvatsikos and Cornell, 2002) and is used in this

paper. Fig. 16 shows the scaled spectral accelerations for the chosen earthquakes as well as the design spectra specified by the IBC (2006).

Incremental dynamic analysis is conducted using the five records. Fig. 17 shows the relationship between the base shear and the roof drift ratio. The maximum lateral capacity of the building shows an over-strength factor varying between 1.90 and 2.16 with an average of 2.03.

At each level of Sa, the ID and the RID for each storey are obtained and compared with the FID and RID corresponding to collapse. Fig. 18a shows the distribution of the ID with time during the dynamic analysis using Northridge record for both the first and the second storey levels. The figure shows that the ID drift of the second storey is higher than the ID of the first storey. The MID and the corresponding RID are equal to 5.14% and 2.80% for the second storey and 4.20% and 2.54% for the first storey. The dashed horizontal lines in the figure define the RID that was calculated as the average value for the last similar cycles of vibrations.

Fig. 18b compares the maximum confined concrete compressive strains for the first and the second storey edge columns. The first storey column is considered crushed as core concrete strain exceeds the crushing strain value calculated using Eq. 12. Although the MID and the corresponding RID of the second storey are higher than those of the first storey (Fig. 18a), its edge column does not experience any crushing and the core concrete strains are very low. This agrees with the limit predicted using the proposed method as the ID for the 1$^{st}$ storey is almost equal to the predicted limit and the ID for the 2$^{nd}$ storey is much lower than the predicted limit. Same performance is observed for all the other columns in these two stories. The following two sections provide an assessment of the building damage as compared to the predicted limits.

### 6.2.1- Building damage based on FID limits

Fig. 19a shows the distribution of MID along the height due to Northridge record (Sa = 2.25g) compared with the proposed FID limits. The damage experienced by the frame is illustrated in Fig. 19b. Reaching the FID limit at the first storey has resulted in excessive damage in only two of its columns. The observed damage in the third floor does not reflect the fact that its MID has reached the FID limit.

Figs. 20 to 23 show similar results for analyses utilizing the earthquake records summarized in table 4. It is clear that reaching the FID limit for the first storey (3.07%) has resulted in severe damage to columns of this storey but has not rendered the frame unstable.

Figures 19 to 23 show the sensitivity of the MID demands to the variability of record-to-record. The storey sustaining the MID has changed from record to another, second storey (Northridge, Imperial Valley, and San Fernando records), first storey (Whittier record), and fifth storey (Loma Prieta record). Figures 22a and 23a show that the ID has non uniform and large dispersion along the height. The ID distribution of Whittier record shows that the MID (3.10%) is at the first storey with a gradual decrease in the values of ID over the building height up reaching the lowest value of 1.09% at the sixth storey. Different scenario for the ID distribution can be observed in case of Loma Prieta record (Fig. 23a) as the distribution is almost constant over the first three storeys (3.00%, 3.20% and 3.06%) with a sudden increase in ID values at the fourth (3.70%) and the fifth storeys (4.89%). These observations make it clear that using a single value of MID is not applicable and will not be able to define local damage. Also they show the significance of the proposed method which allows comparing the seismic ID demands by specific FID for each storey to predict the local and the global damage states.

**6.2.2- Building damage based on the RID limits**

Figure 19c shows the distribution of RID along the height due to Northridge record (Sa = 2.60g) compared with the RID collapse limits estimated by the proposed method. The damage experienced is illustrated in Fig. 19d. Reaching the collapse limit for RID at the first storey (Fig. 19c) causes excessive damage to four of its columns (Fig 19d). Two of the third storey columns reached the crushing strain at their top end. The RID at this storey is about 1.9% compared to a collapse limit of RID = 3.23% which indicates that the RID provided better prediction than FID for this floor behaviour.

Figs. 20 to 23 show similar results for analyses utilizing remaining earthquake records. For all records, severe damage is observed in the first storey columns due to reaching the RID limit (2.53%) and the RC frame can be considered at failure state. The distribution of the RID in case of Loma Prieta record shows contribution of higher modes as the RID is almost the same for the first five stories.

Figures 19 to 23 show the sensitivity of the RID demands to the variability of record-to-record. The storey sustaining the maximum RID has changed from record to record, second storey (Northridge, Imperial Valley, and Loma Prieta records) and first storey (San Fernando and Whittier earthquakes). This is matching what was concluded by Ruiz-Garcia and Miranda (2006). Figures 22c and 23c confirm the idea of Medina and Krawinkler (2003) that the RID has non uniform and large dispersion along the height. For Whittier record, RID reached values of 2.50%, 1.30%, and less than 0.60% for the first, second, and remaining storeys, respectively. Different scenario for the RID distribution can be observed in case of Loma Prieta record (Fig. 23c) as the distribution is almost constant over the full height. These observations make it clear that using a single value of maximum RID is not applicable and will not be able to define local damage. Also they show the significance of the proposed method which allows comparing the seismic RID demands by specific residual drift limit for each storey to predict the local damage and the global damage states.

## 7- Conclusions

In this paper, a simplified method to define the collapse limits in terms of FID and RID is presented. The method takes into consideration the change in columns ductility due to the change of axial load. The method was validated using analytical and experimental work by others. The validation showed that the method was capable to predict accurately both the value of ID causing collapse and the location of maximum damage. A six-storey RC structure is considered as a case study. The building is analyzed using the proposed method to estimate its collapse limits. The building is then subjected to static pushover analysis and nonlinear dynamic analysis using five earthquake records. The six-storey building results showed that the predicted FID and RID limits can be reliable in identifying critical stories. The results obtained from the pushover analysis for the six-storey building showed that the proposed method explains accurately the damage profile of the building. Also the results confirmed that using a single value for MID or maximum RID cannot identify the position of the critical damage of the building.

Results obtained from the dynamic analysis led to the following conclusions:

1) FID limits predicted by the proposed method were conservative as reaching these limits do not lead to reaching a failure state. Using these limits defined accurately the storey experiencing the highest damage.
2) Using the RID collapse limits accurately represented the building failure state and locations of local damage. During the analyses the collapse occurred due to reaching the collapse limit of

the first storey level (2.53% RID). This shows that the collapse prevention limit proposed by the FEMA 273 (4% RID) is unconservative.

3) The building damage under the effect of all earthquakes showed that columns are more susceptible to concrete crushing when compared to beams. This might be due to the low level of axial forces acting on the beams.
4) For all the ground motion records used in the analysis, predictions of the proposed method were acceptable. The method can be used following an earthquake to predict the location of the critical damage by comparing its predicted limits for RID with the measured RID. This can help engineers to quickly identify the critical stories and the positions of the expected damage.

Conclusions of this paper are limited to the studied frames, and thus further validation for the proposed method is required.

**List of abbreviations and symbols**

| | |
|---|---|
| RC | Reinforced Concrete |
| MID | Maximum Inter-storey Drift |
| ID | Inter-storey Drift |
| PGA | Peak Ground Acceleration |
| RID | Residual Inter-storey Drift |
| $V_f$ | Column shear for a column fully restrained against rotation |
| $E_c$ | Modulus of elasticity for columns |
| $I_c$ | Column moment of inertia |
| $I_b$ | Beam moment of inertia |
| h | Column height |
| $\Delta$ | Inter-storey drift |
| $V_i$ | Shear force for partially restrained columns |
| $\alpha$ | Reduction factor for the lateral stiffness |
| $\theta$ | Joints rotation |
| $M_F$ | Fixed end moment |
| $d_{ct}$ | Moment distribution factor |
| $E_b$ | Modulus of elasticity for beams |
| $M_{ct}$ | Moment acting at the top of the column |
| $M_{cb}$ | Moment acting at the bottom of the column |
| $m_{av}$ | Storey drift magnification factor |
| $\varepsilon_y$ | Yielding strain |
| $\varepsilon_{cu(\text{confined concrete})}$ | Confined concrete ultimate strain |
| $\varepsilon_{cu(\text{unconfined concrete})}$ | Unconfined concrete ultimate strain |
| $\rho_s$ | Ratio of the volume of transverse reinforcement to the volume of concrete core. |
| $f_y$ | Steel yielding stress. |
| $\varepsilon_{sm}$ | Steel strain at maximum tensile stress. |
| $K_h$ | Confinement factor. |
| FID | Failure Inter-storey Drift. |

**Acknowledgements**

This research was funded by the National Sciences and Engineering Research Council of Canada (NSERC). ZEUS-NL was developed at the Mid-America Earthquake Center using the National Science Foundation Award Number EEC-9701785.

**References**

Abrams, D.P., 1987, "Influence of axial force variation on flexural behavior of reinforced concrete columns", *ACI Structural Journal* 84(3), 246–54.

ACI 318, 2005, "Building code requirements for structural concrete (ACI 318-05) and commentary (ACI 318R-05)", American Concrete Institute, Farmington Hills MI, USA, 430 pp.

Bazzurro, P., Cornell, C.A., Menun, C.A., and Motahari, M., 2004, "Guidelines for seismic assessment of damaged buildings", *Proc. of the Thirteenth World Conference on Earthquake Engineering*, Vancouver, BC, Canada, Paper No. 1708, 15 pp.

Broderick, B.M. and Elnashai, A.S., 1994, "Seismic resistance of composite beam-columns in multi-storey structures, Part 2: Analytical model and discussion of results", *Construction Steel Research* 30(3), 231–258.

Christopoulos, C., Pampanin, S. and Priestley, M.J.N., 2003, "Performance-based seismic response of framed structures including residual deformations, Part I: single-degree-of-freedom systems", *Journal of Earthquake Engineering* 7(1), 97–118.

Dymiotis, C., 2000, "Probabilistic seismic assessment of reinforced concrete buildings with and without masonry infills", Ph.D. thesis, Imperial College of Science, Technology and Medicine, London, UK.

Elnashai, A.S., Papanikolaou, V. and Lee, D.H., 2002, "ZEUS-NL user manual," Civil and Environmental Engineering Department, University of Illinois at Urbana–Champaign, Mid-America Earthquake Center, Urbana, IL, USA.

Eurocode 8, 1994, "Design provisions for earthquake resistance of structures", Comité Européen de Normalisation, European Commission for standardization Brussels, Belgium.

FEMA 273, 1997, "NEHRP Guidelines for the Seismic Rehabilitation of Buildings", Federal Emergency Management Agency, Washington, DC, USA.

Ghobarah, A., Aly, N.M., El-Attar, M., 1998, "Seismic reliability assessment of existing reinforced concrete building", *Journal of Earthquake Engineering* 2(4), 569-592.

Ghobarah, A., Abou-Elfath, H., and Biddah, A., 1999, "Response-based damage assessment of structures", *Journal of Earthquake Engineering and Structural Dynamics* 28(1), 79-104.

Haselton, C.B. and Deierlein, G.G., 2008, "Assessing seismic collapse safety of modern reinforced concrete moment frame buildings", Report PEER 2007/08, Pacific Earthquake Engineering Research Center, University of California at Berkeley, Berkeley, CA, USA, 274 pp.

IBC, 2006, International Building Code, International Code Council, ICC, Country Club Hills, IL, USA, 679 pp.

Jeong, S.H., and Elnashai, A., 2005, "Analytical assessment of an irregular RC frame for full-scale 3D pseudo-dynamic testing part I: analytical model verification", *Earthquake Engineering* 9(1), 95-128.

Kappos, A.J., 1997, "A comparative assessment of R/C structures designed to the 1995 Eurocode 8 and the 1985 CEB seismic code", *The Structural Design of Tall Buildings* 6(1), 59-83.

Lee, D., Choi, E. and Zi, G., 2005, "Evaluation of earthquake deformation and performance for RC bridge piers", *Engineering Structures* 27(10), 1451-1464.

Lu, Y., 2002, "Comparative study of seismic behaviour of multistory reinforced concrete framed structures", *Journal of Structural Engineering* 128(2), 169-178.

MacGregor, J.G. and Wight, J.K., 2005, "*Reinforced Concrete Mechanics and Design"*, Prentice Hall, Upper Saddle River, NJ, USA.

MacRae, G.A., Kawashima, K., 1997, "Post-earthquake residual displacements of bilinear oscillators", *Earthquake Engineering and Structural Dynamics* 26(7), 701–716.

Mander, J.B., Priestley, M.J.N., Park, R., 1988, "Theoretical Stress-Strain Model for Confined Concrete", ASCE Journal of Structural Engineering 114(8), 1804-1826.

Medina, R. and Krawinkler, H. 2003, "Seismic demands for non-deteriorating frame structures and their dependence on ground motions", Report PEER 2003/15, Pacific Earthquake Engineering Research Center, University of California at Berkeley, Berkeley, CA, USA, 335 pp.

Moehle, J., Ghannoum, W. and Bozorgnia, Y., 2005, "Collapse of lightly confined reinforced concrete frames during earthquakes", *Proc. - NATO Science for Peace Workshop in Advances in Earthquake Engineering for Urban Risk Reduction*, Istanbul, Turkey, 317-332.

Muto, K., 1974, "*A Seismic Design Analysis of Buildings"*, Maruzen Company Ltd., Tokyo, Japan.

Mwafy, A.M. and Elnashai, A.S., 2001, "Static pushover versus dynamic collapse analysis of RC buildings", *Engineering Structures* 23(5), 407-424.

Paulay, T. and Priestley, M.J.N., 2009, "*Seismic Design of Reinforced Concrete and Masonry Buildings"*, John Wiley & Sons Inc., Hoboken, NJ, USA.

Roufaiel, M.S.L., and Meyer, C., 1983, "Analysis of damaged concrete frame buildings", Report NSF-CEE 81-21359-1, Department of Civil Engineering and Engineering Mechanics, Columbia University, New York, NY, USA.

Ruiz-Garcia, J., Miranda E., 2006, "Residual displacement ratios for assessment of existing structures", *Earthquake Engineering and Structural Dynamics* 35(3), 315–336.

Sakai, J. and Mahin, S.A., 2004, "Analytical investigations of new methods for reducing residual displacements of reinforced concrete bridge columns", PEER-2004/02, Pacific Earthquake Engineering Research Center, Univ. of California at Berkeley, California, USA, 291 pp.

Sakai, J. and Mahin S., 2005, "Earthquake simulator tests on the mitigation of residual displacement of reinforced concrete bridge columns", *Proc., 21st US-Japan Bridge Engineering Workshop*, Tsukuba Japan, October 2005, 8 pp.

SEAOC, 1995, "Performance based seismic engineering of buildings", Vision 2000 Committee, Structural Engineering Association of California, Sacramento, CA, USA.

Shome, N., Cornell, C.A., 1999, "Probabilistic seismic demand analysis of non-linear structures", Report No. RMS-35, RMS Program, Stanford University, Stanford, CA, USA.

Sozen, M.A., 1981, "Review of earthquake response of reinforced concrete buildings with a view to drift control", *State-of-the-Art in Earthquake Engineering*, Turkish National Committee on Earthquake Engineering, Istanbul, Turkey, pp. 383-418.

Stephens, J.E. and Yao, J.T.P., 1987, "Damage assessment using response measurements", *Journal of Structural Engineering, ASCE* 113(4), 787-801.

Toussi, S. and Yao, J.T.P., 1982, "Hysteresis identification of existing structures", *Journal of Engineering Mechanics, ASCE* 109(5), 1189-1203.

Vamvatsikos, D. and Cornell, C. A., 2002, "Incremental dynamic analysis", *Journal of Earthquake Engineering and Structural Dynamics* 31(3), 491-514.

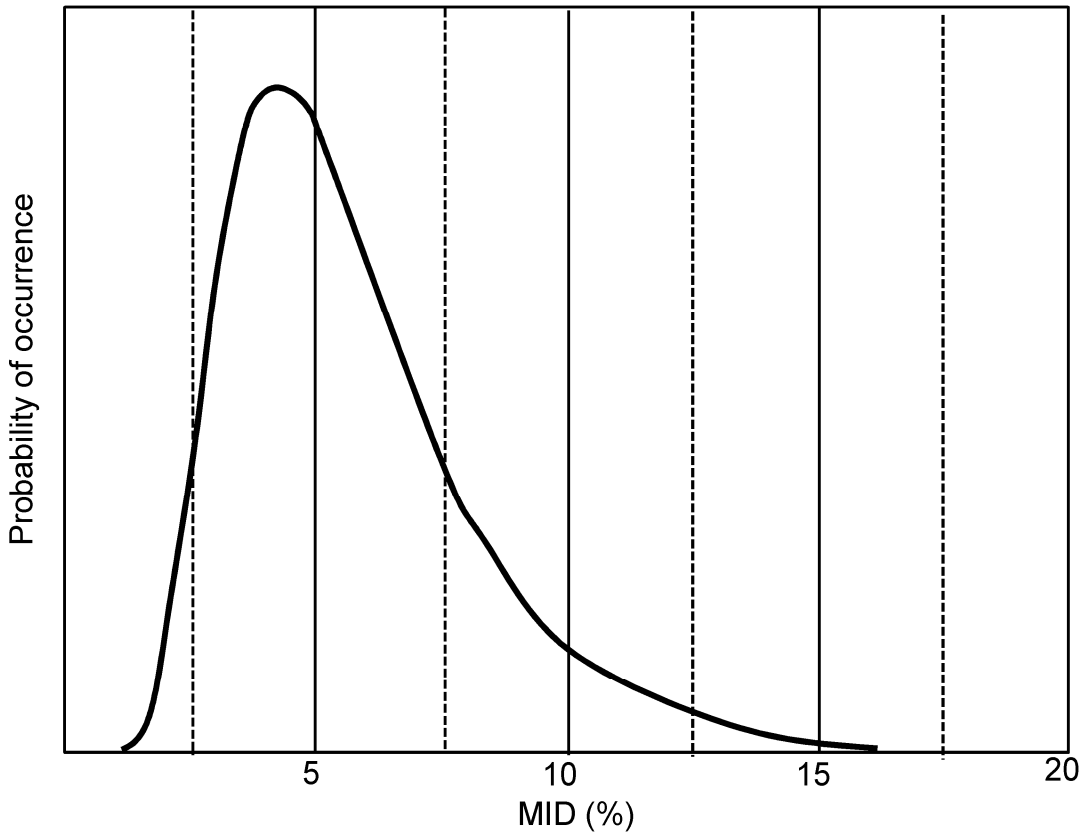


Figure 1: Statistical distribution of experimentally obtained MID.

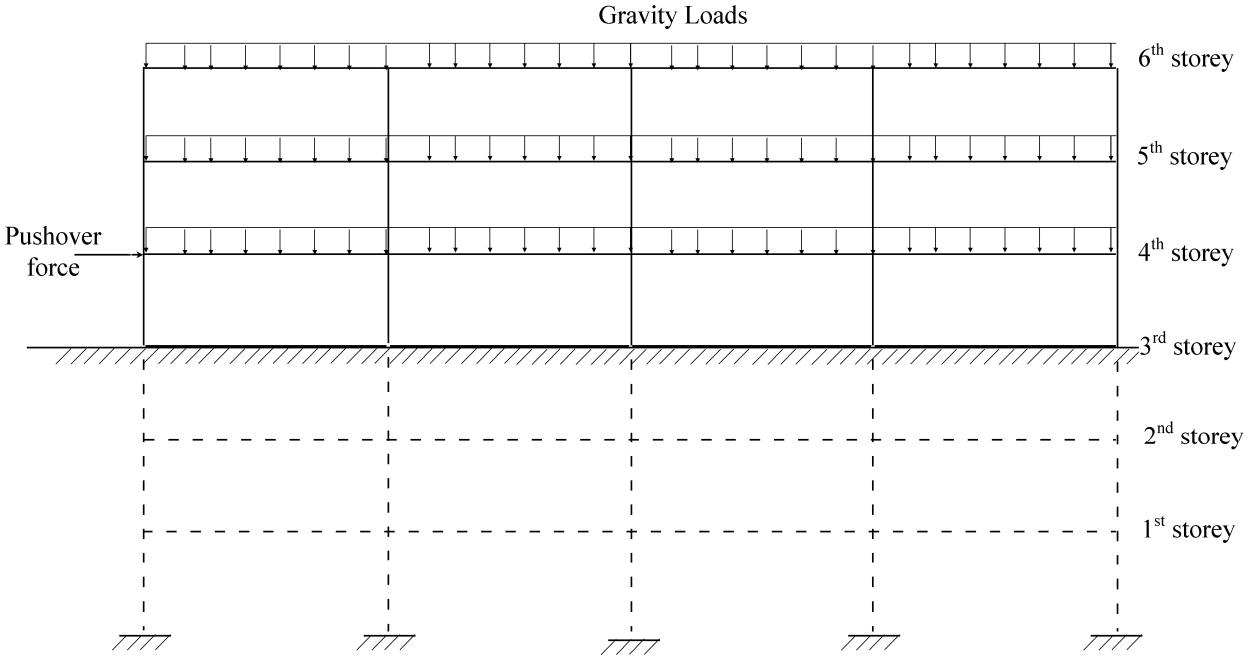


Figure 2: Proposed method to estimate inter-storey drift limits for the fourth storey of a six-storey building.

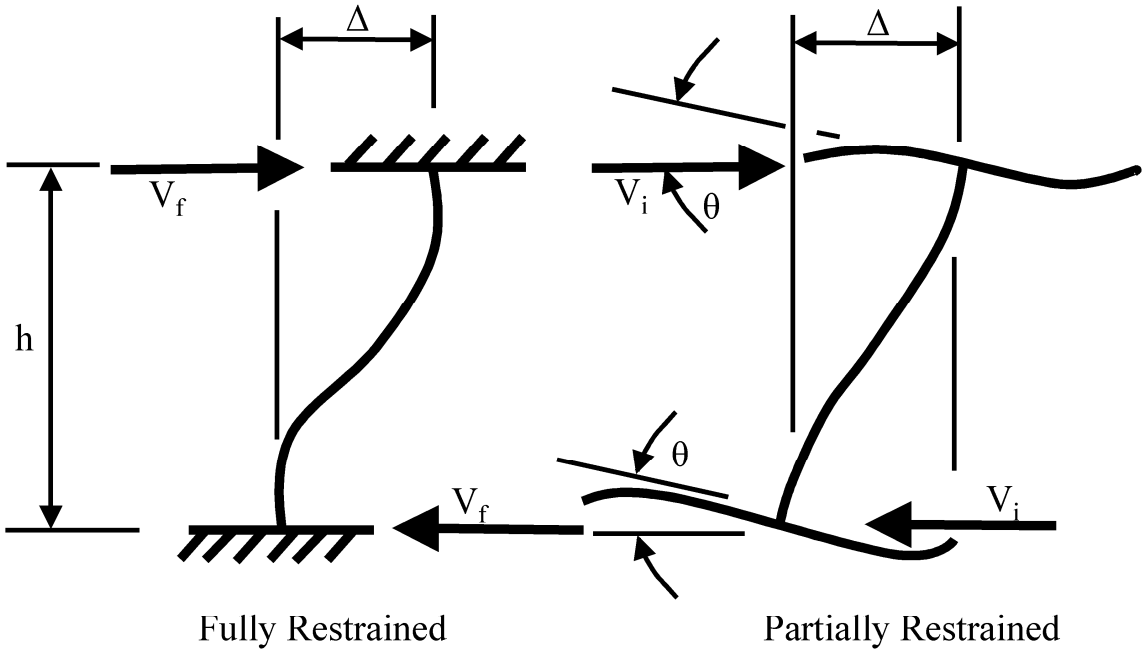


Figure 3: Shear forces induced by relative storey drifts (Paulay and Priestley, 2009).

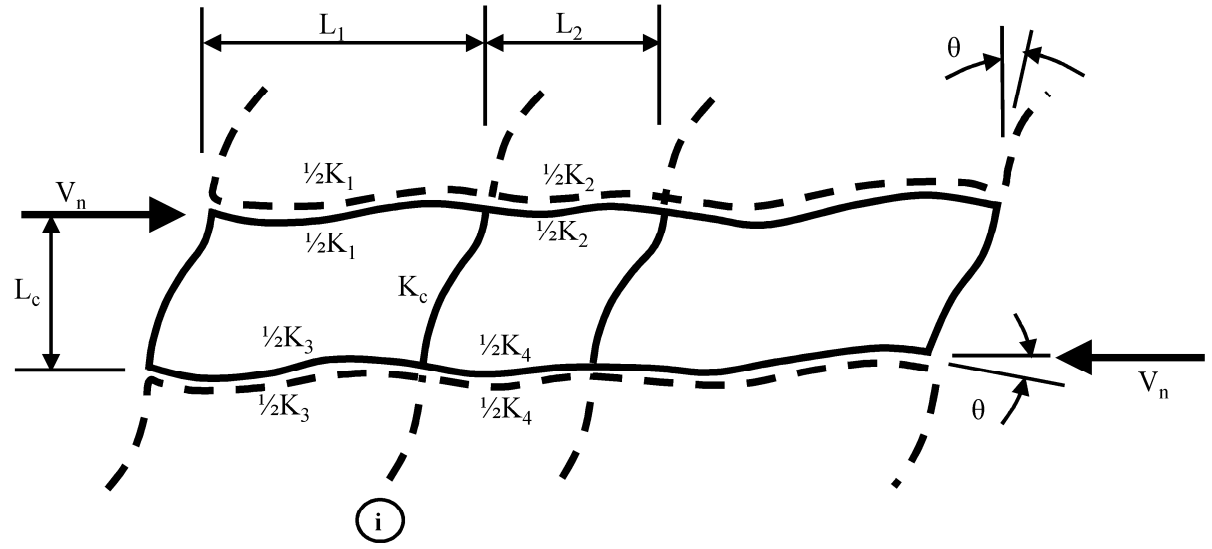


Figure 4: Simplified sub-frame used for lateral force analysis (Paulay and Priestley, 2009).

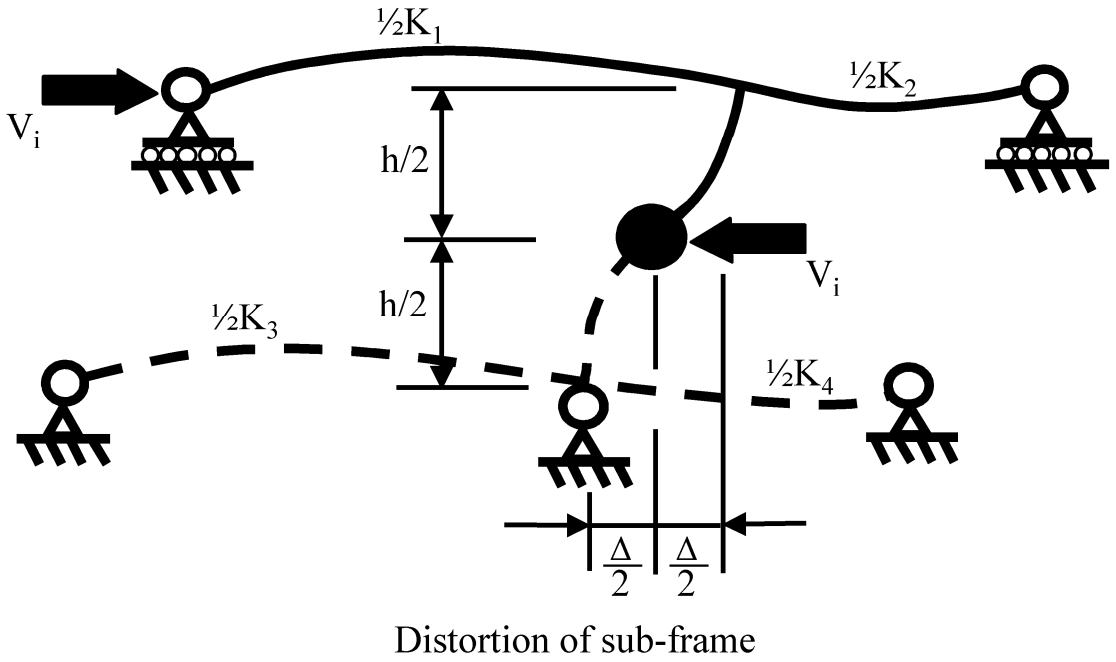


Figure 5: Isolated column and restraining beams (Paulay and Priestley, 2009).

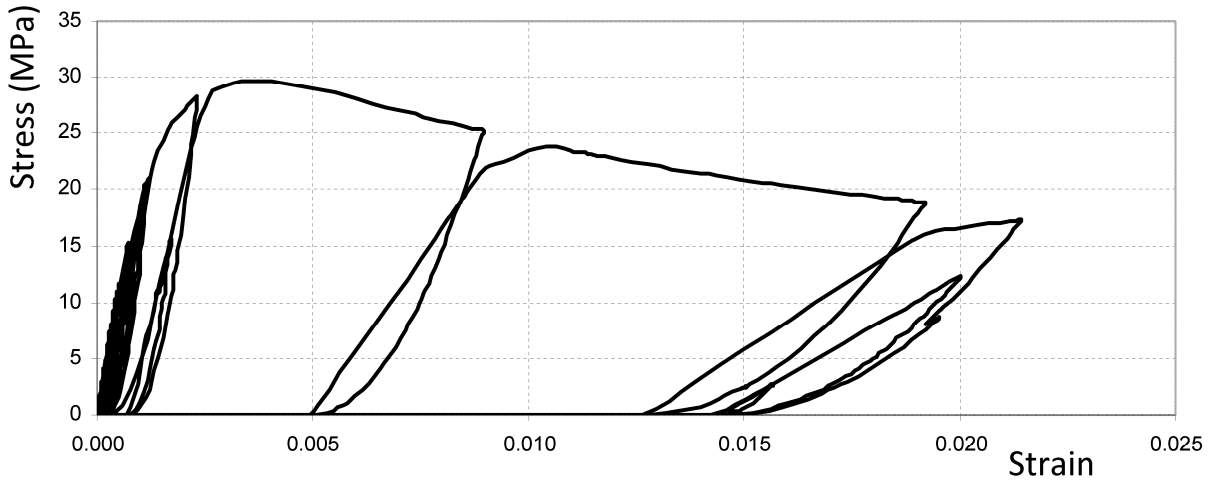


Figure 6: Stress-strain curve of confined concrete.

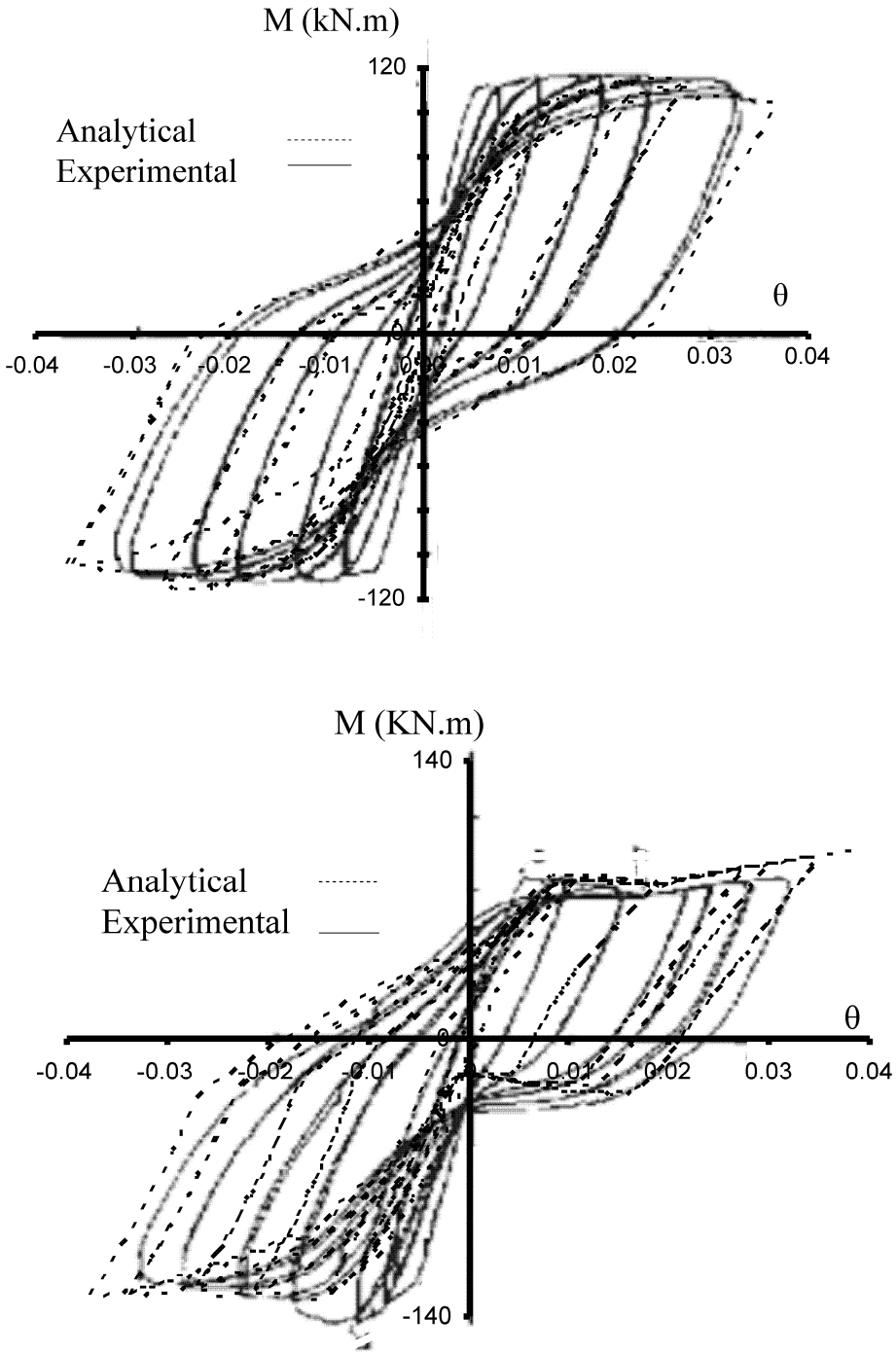


Figure 7: Moment-rotation relationship of a RC column under cyclic lateral displacements.

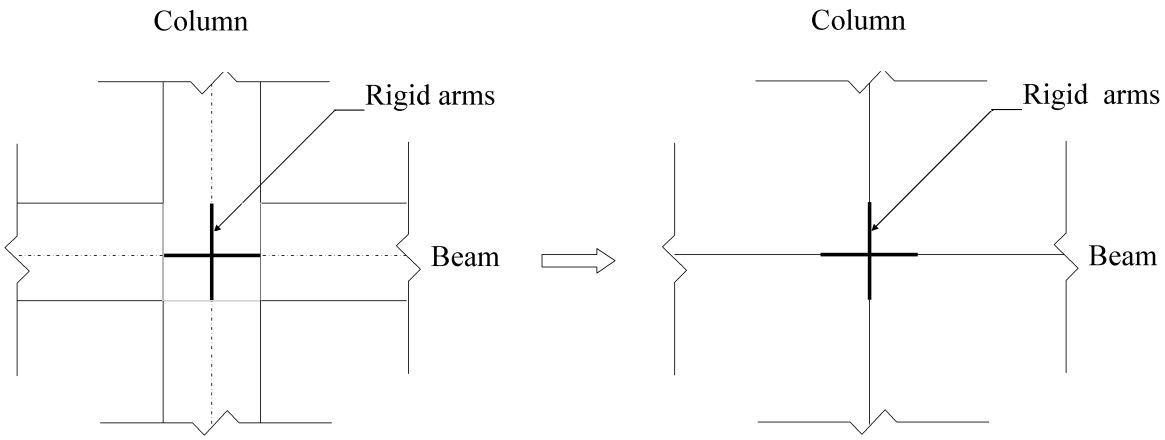


Figure 8: Rigid arms for modeling an interior beam-column connection.


Figure 9: Estimated collapse ID limits compared with experimental results by Lu (2002).

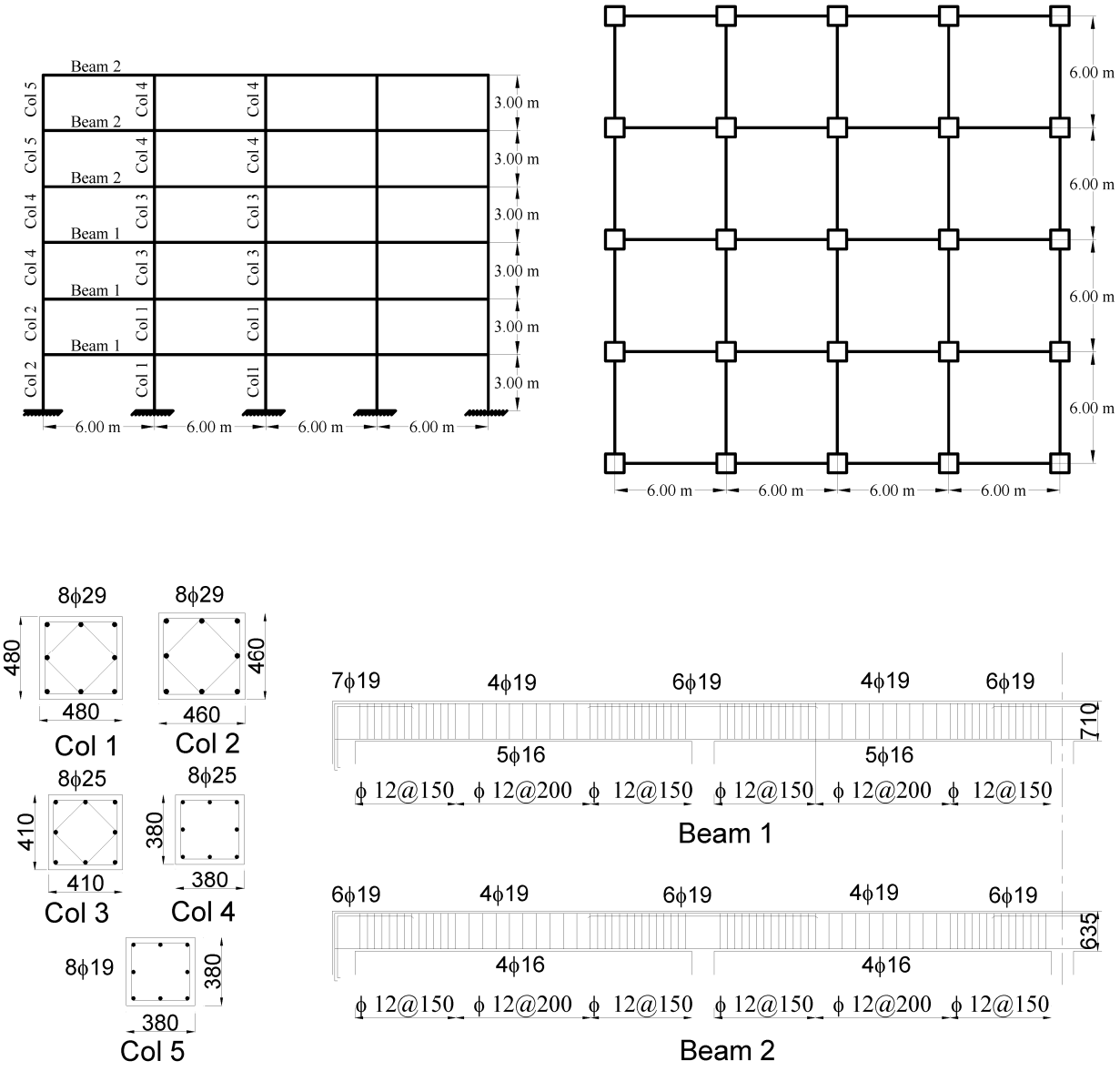


Figure 10: Six-storey RC building.

a) Plan and elevation
b) Details of reinforcement

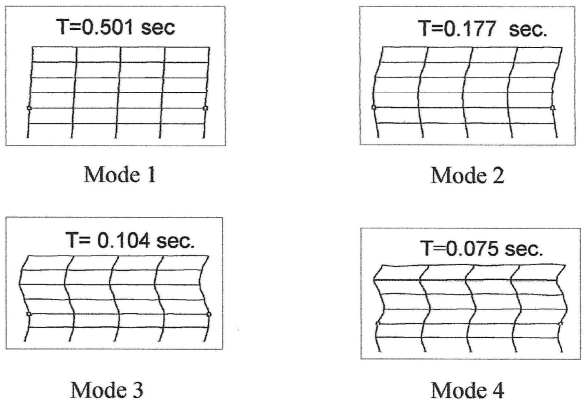


Figure 11: First four mode shapes of the six-storey RC building.

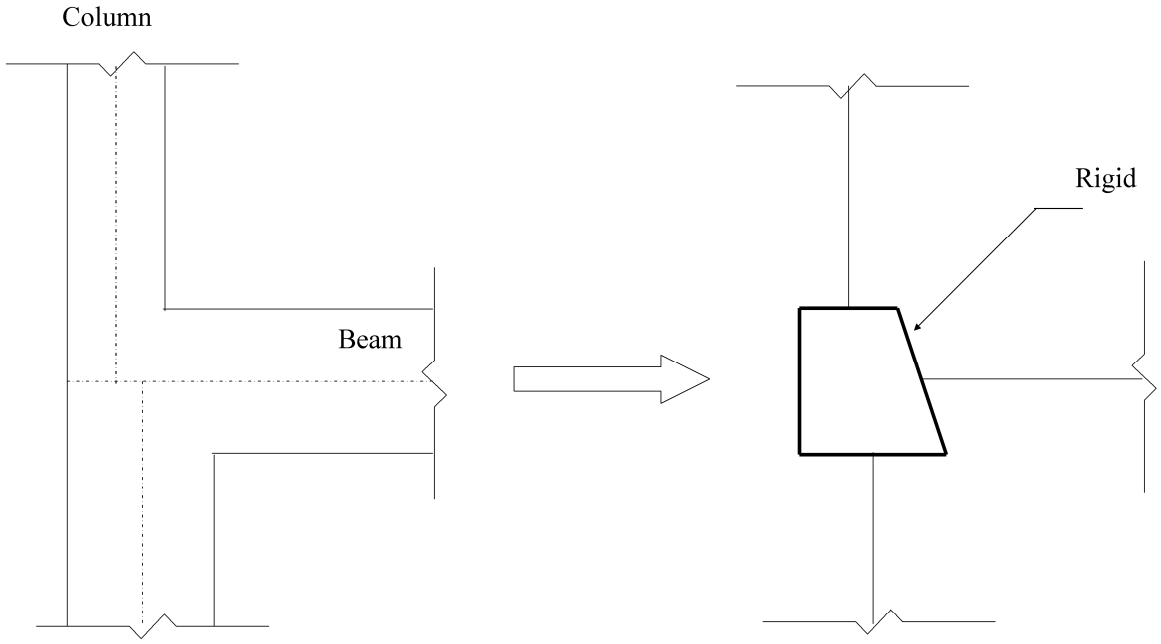


Figure 12: Modeling an edge beam-column connection.

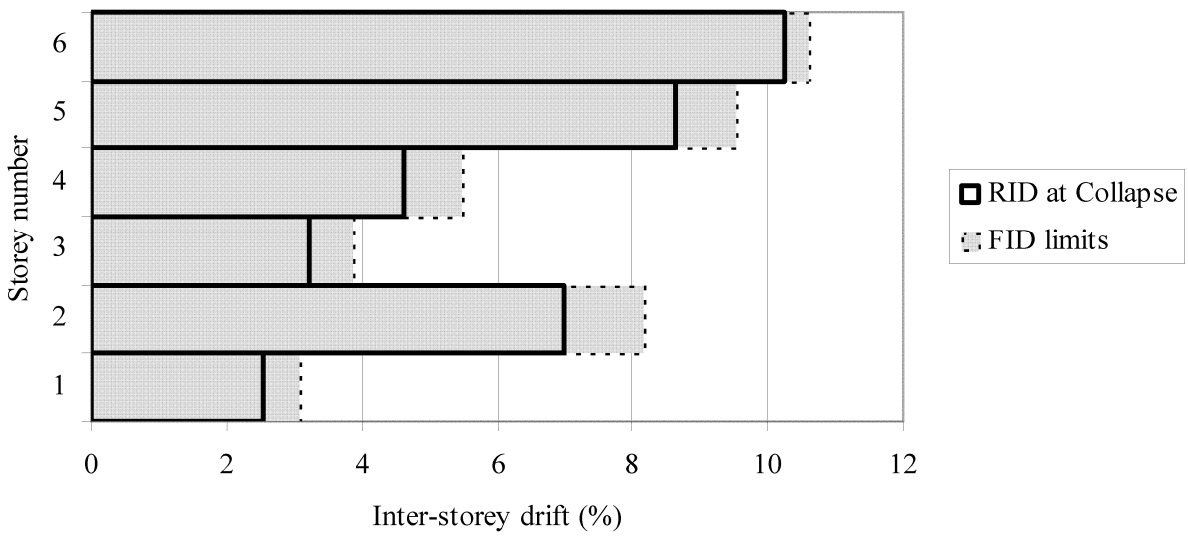


Figure 13: Proposed FID limits and the corresponding RID limits for the six-storey building.

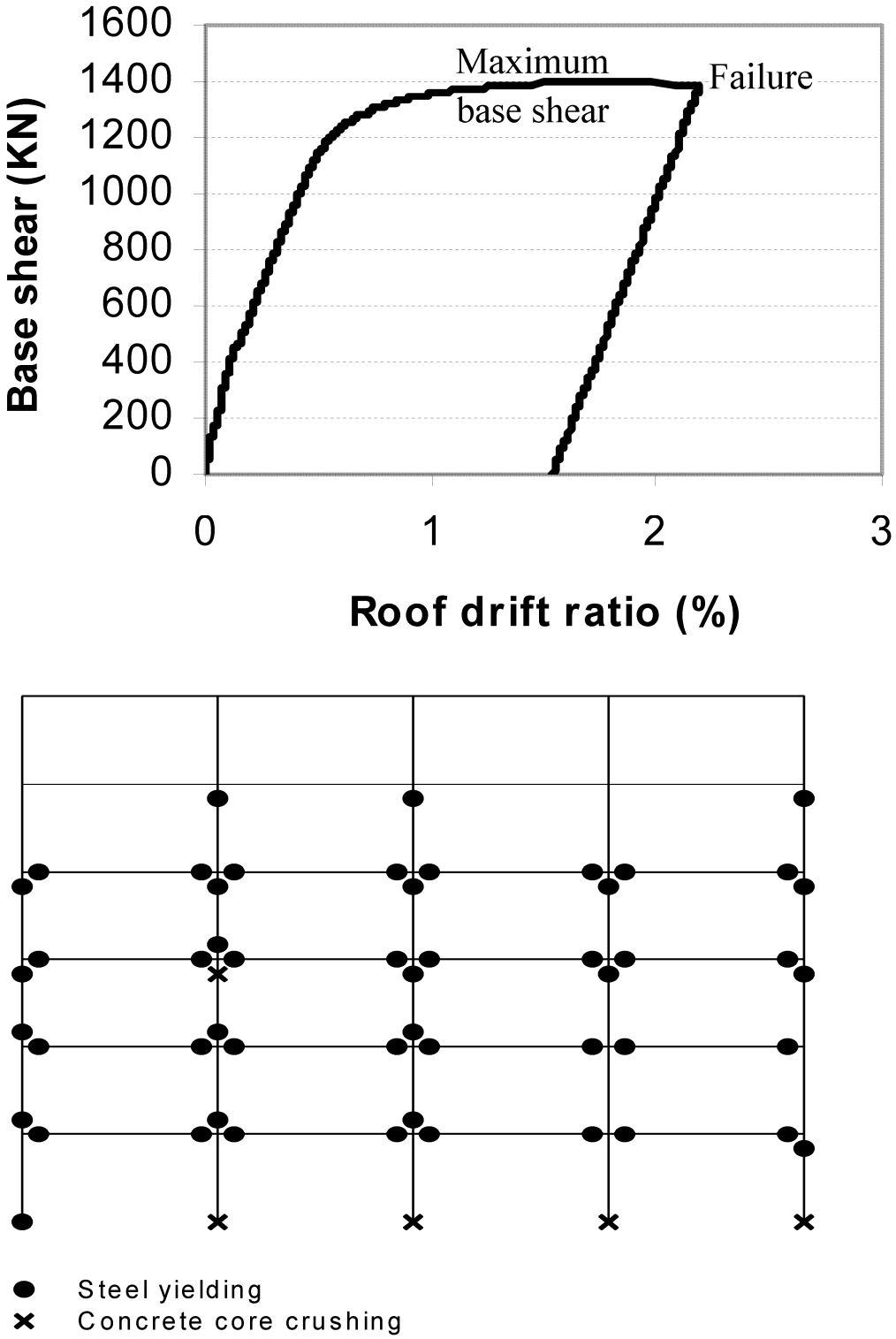


Figure 14: Pushover analysis results.

a) Relationship between roof drift and base shear
b) Observed damage at failure

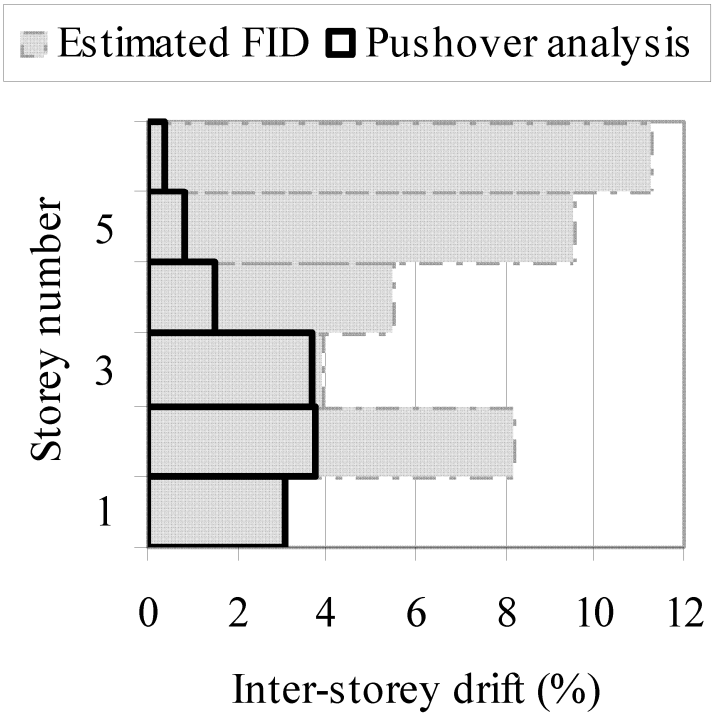


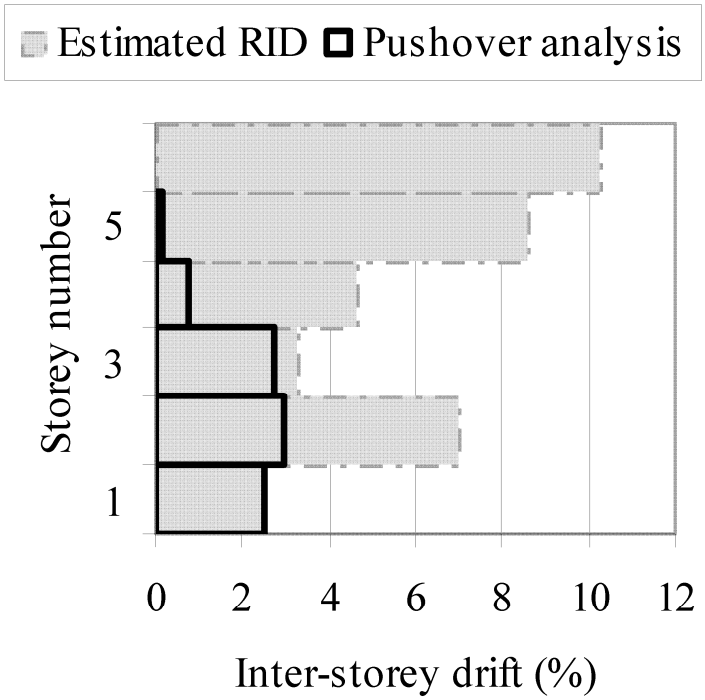


Figure 15: ID obtained using pushover analysis as compared to the proposed collapse limits.

a) Pushover ID and FID limits
b) Pushover RID and RID limits

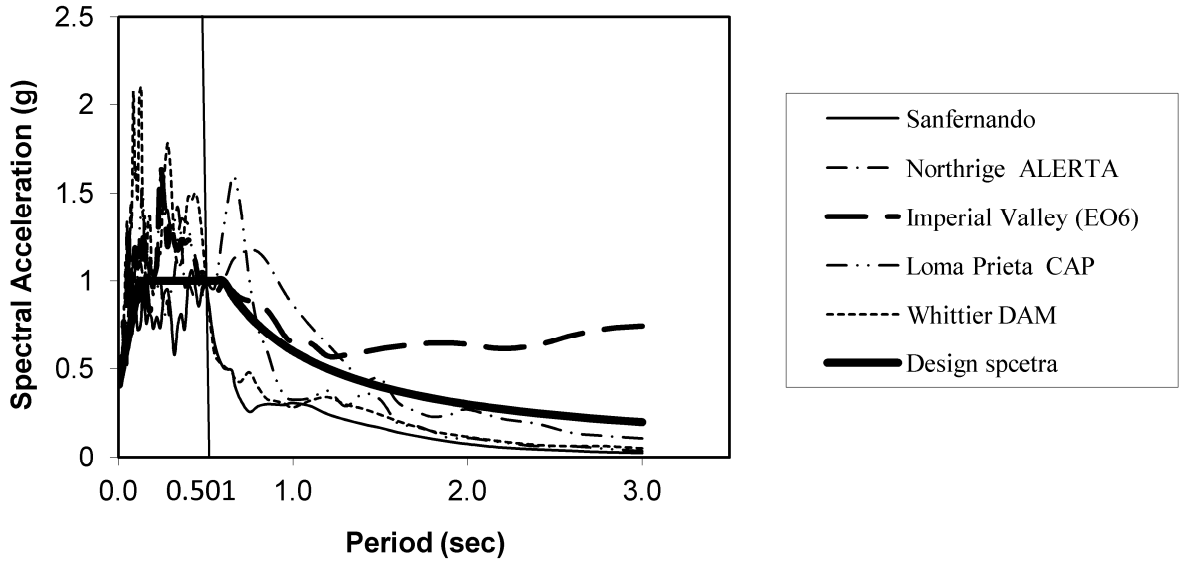


Figure 16: Spectral acceleration for the horizontal seismic components and the design spectra.

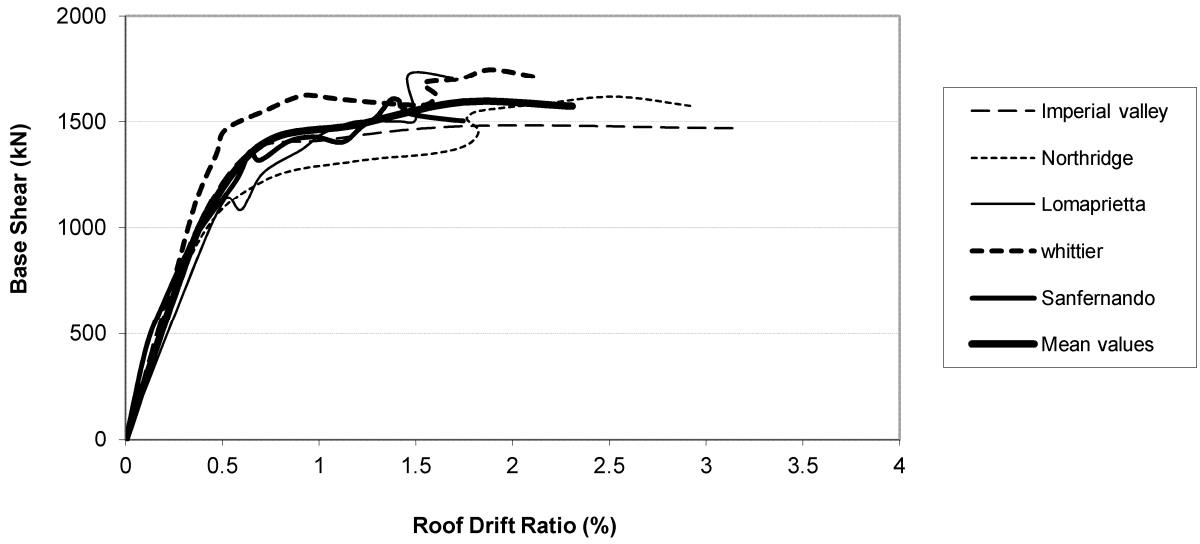


Figure 17: Relationship between the base shear and the roof drift ratio obtained from the IDA.

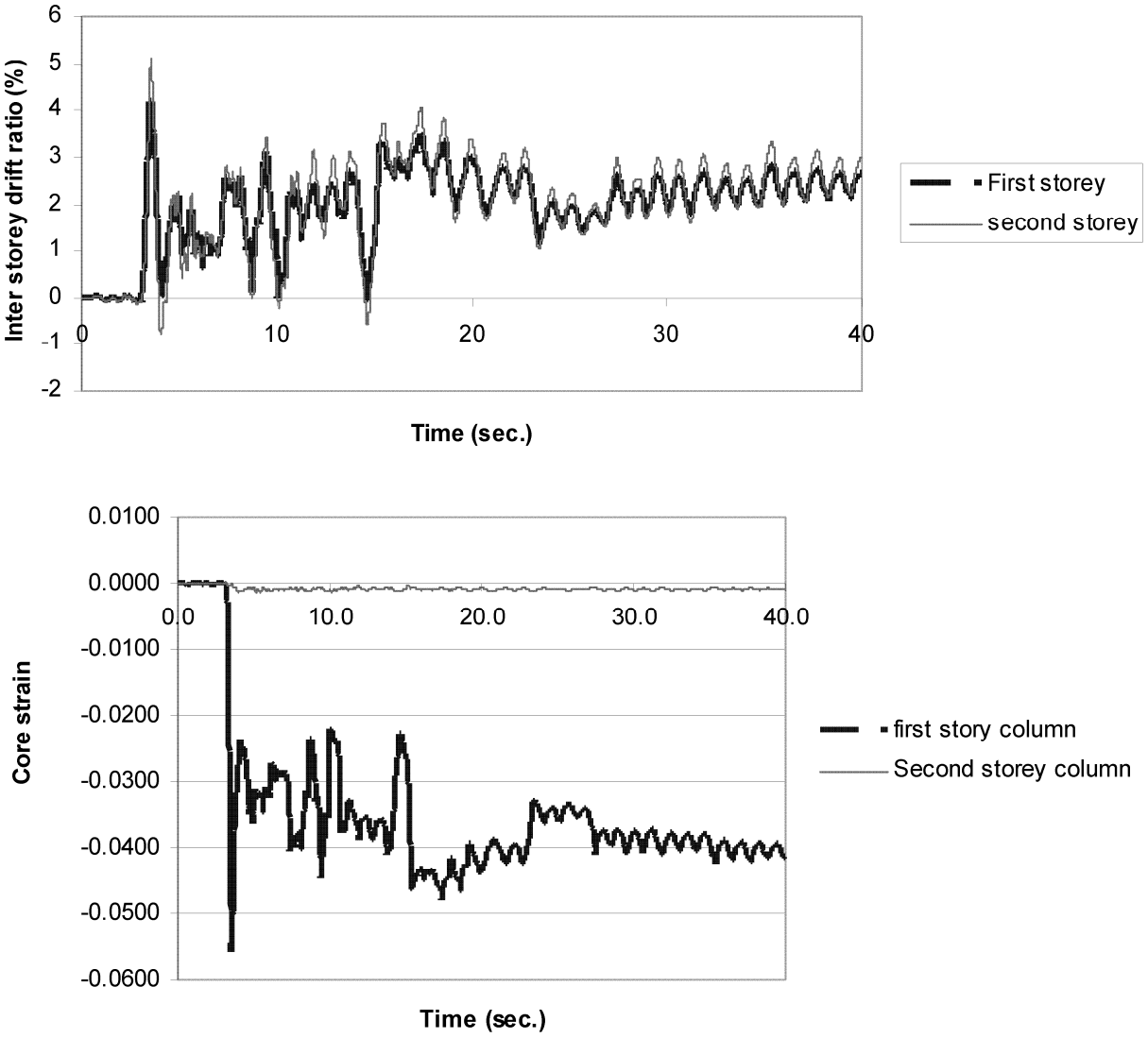


Figure 18: RID and column compressive strains during Northridge earthquake.

a) RID in the first and second stories
b) Confined concrete compressive strain in the columns of the first and second stories

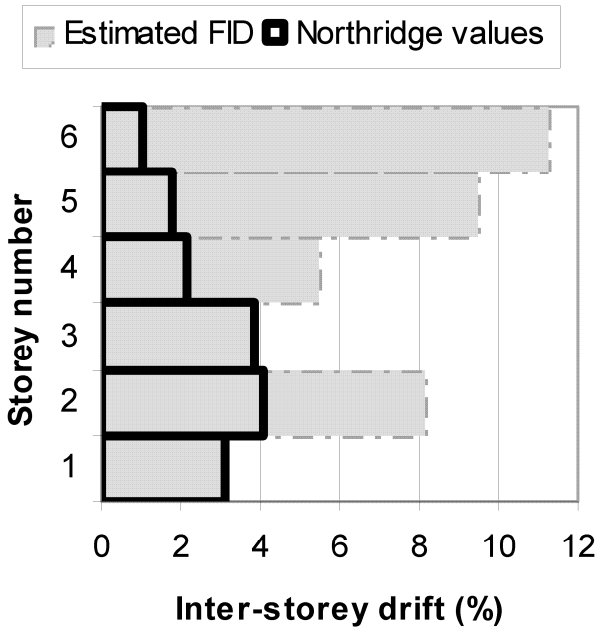


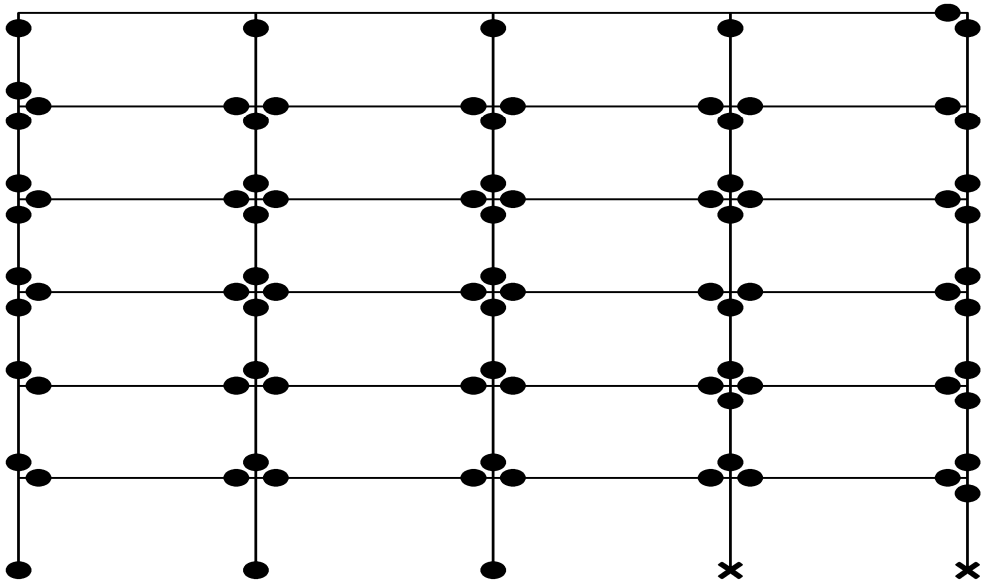

Steel yielding
Concrete core crushing

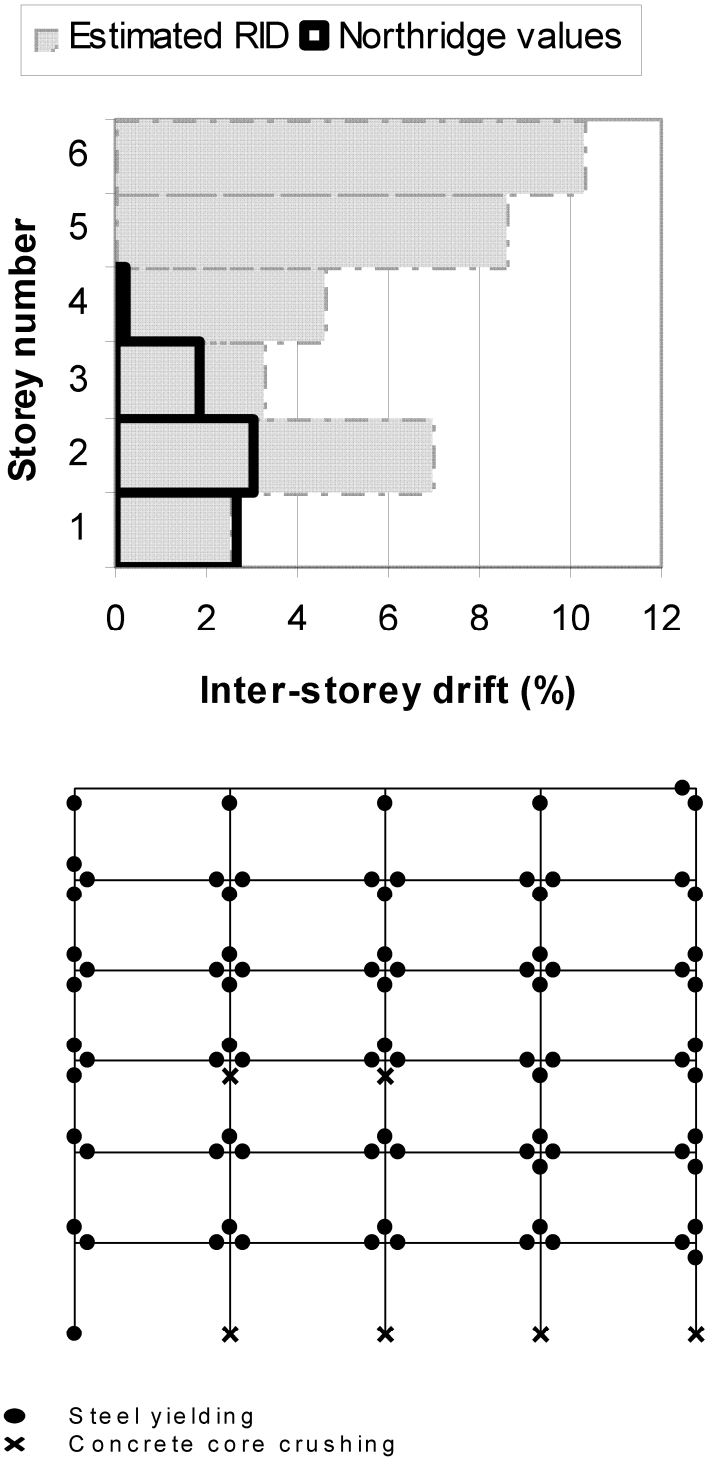


Figure 19: Results considering Northridge earthquake.

a) MIDs at Sa = 2.25g as compared to FID limits
b) Distribution of yielding and crushing at FID limit
c) RIDs at Sa = 2.60g as compared to RID limits
d) Distribution of yielding and crushing at RID limit

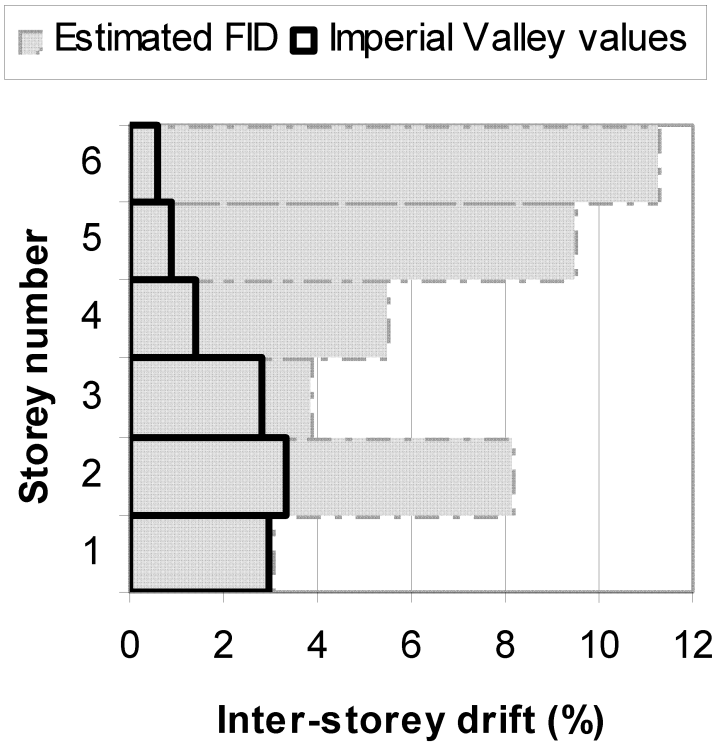


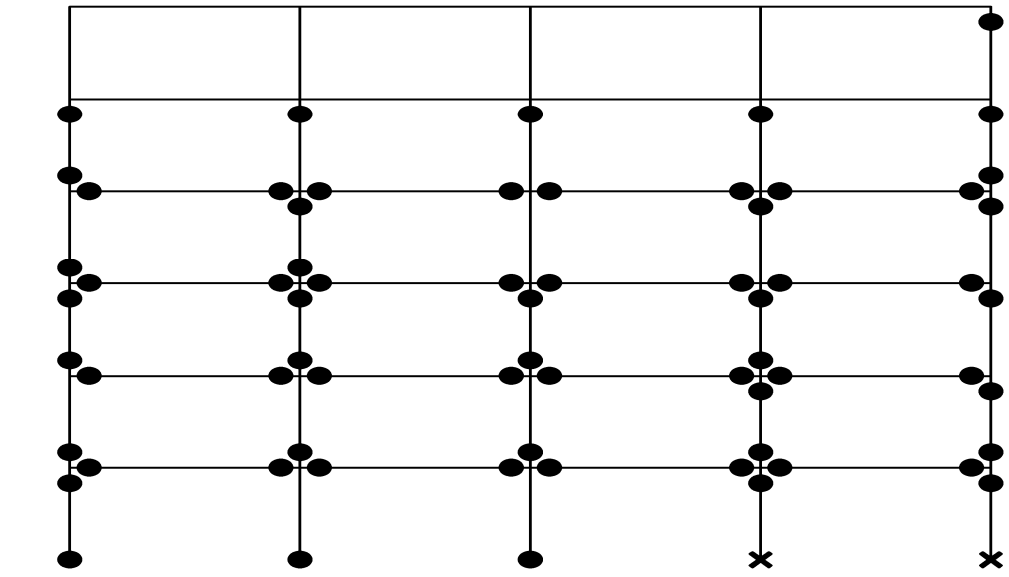

Steel yielding
Concrete core crushing

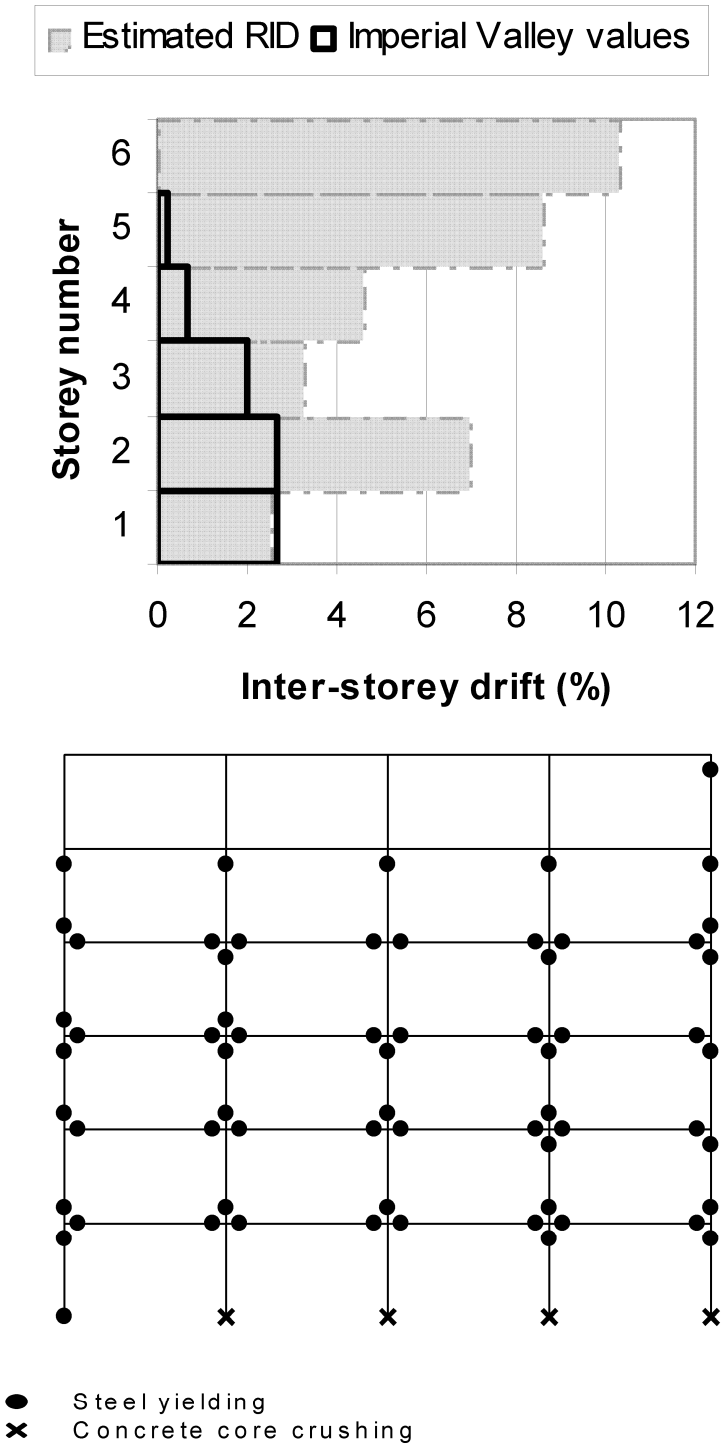


Figure 20: Results considering Imperial Valley earthquake.

a) MIDs at Sa = 1.03g as compared to FID limits
b) Distribution of yielding and crushing at FID limit
c) RIDs at Sa = 1.15g as compared to RID limits
d) Distribution of yielding and crushing at RID limit

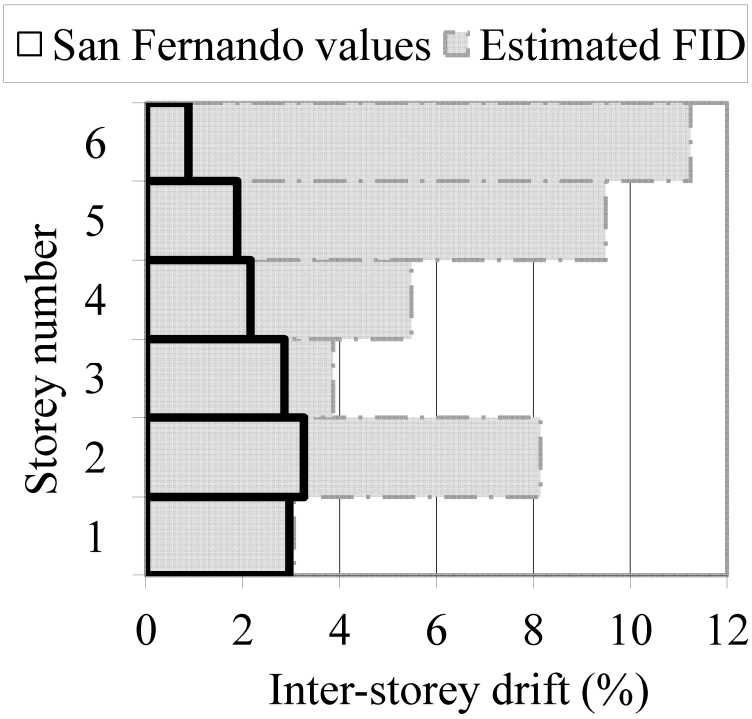
San Fernando values
Estimated FID
Storey number
6
5
4
3
2
1
0
2
4
6
8
10
12
Inter-storey drift (%)

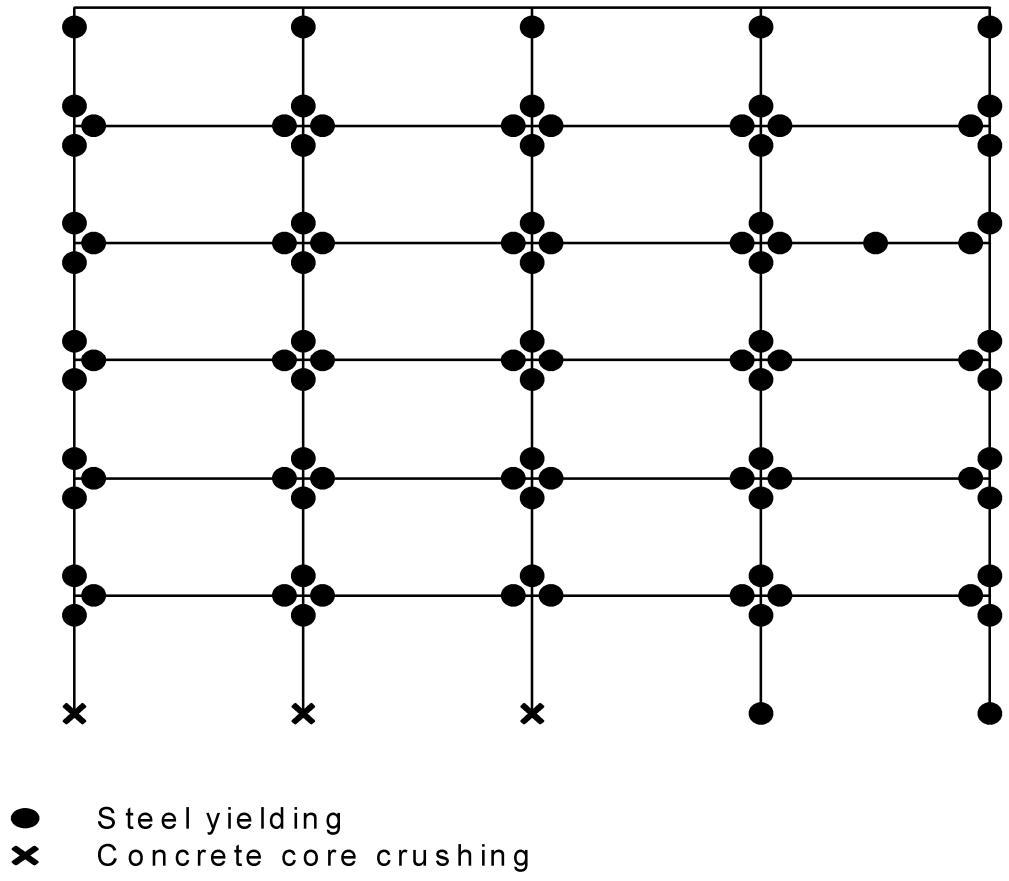
Steel yielding
Concrete core crushing

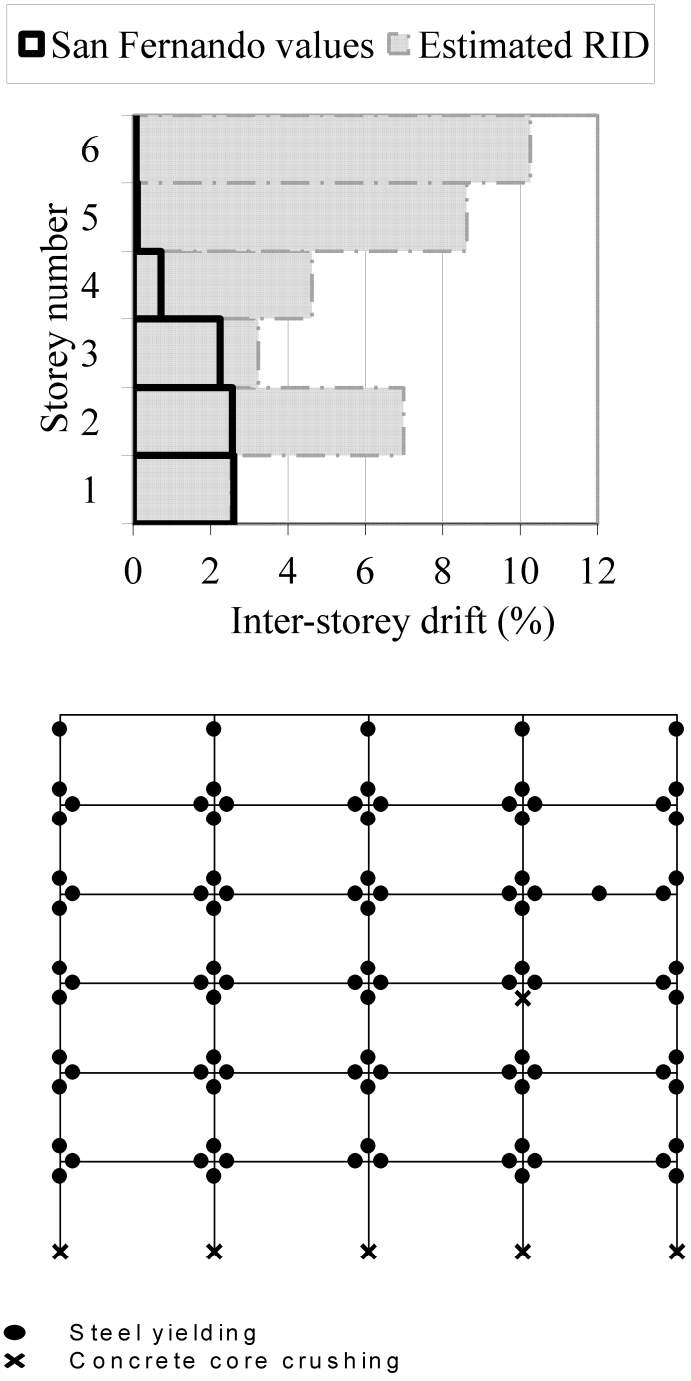


Figure 21: Results considering San Fernando earthquake.

a) MIDs at Sa = 4.85g as compared to FID limits
b) Distribution of yielding and crushing at FID limit
c) RIDs at Sa = 8.15g as compared to RID limits
d) Distribution of yielding and crushing at RID limit

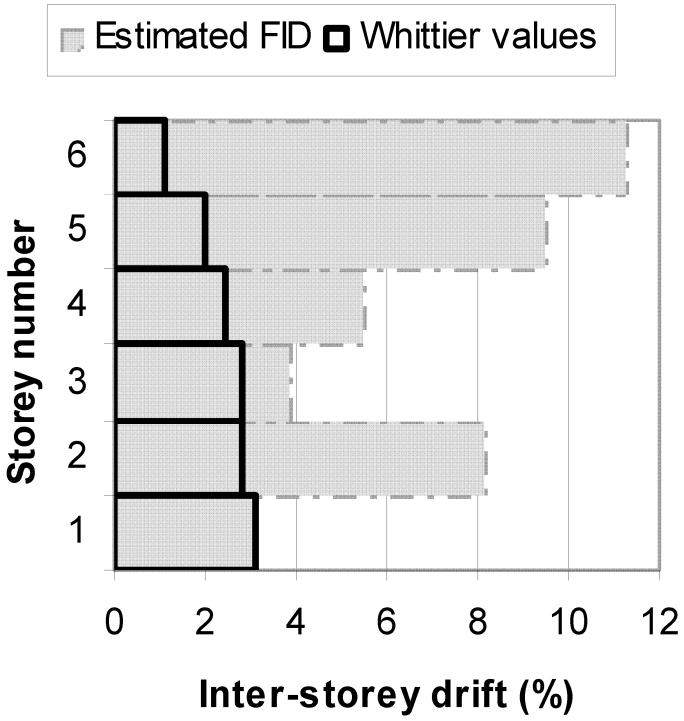
Estimated FID
Whittier values
Storey number
6
5
4
3
2
1
0
2
4
6
8
10
12
Inter-storey drift (%)

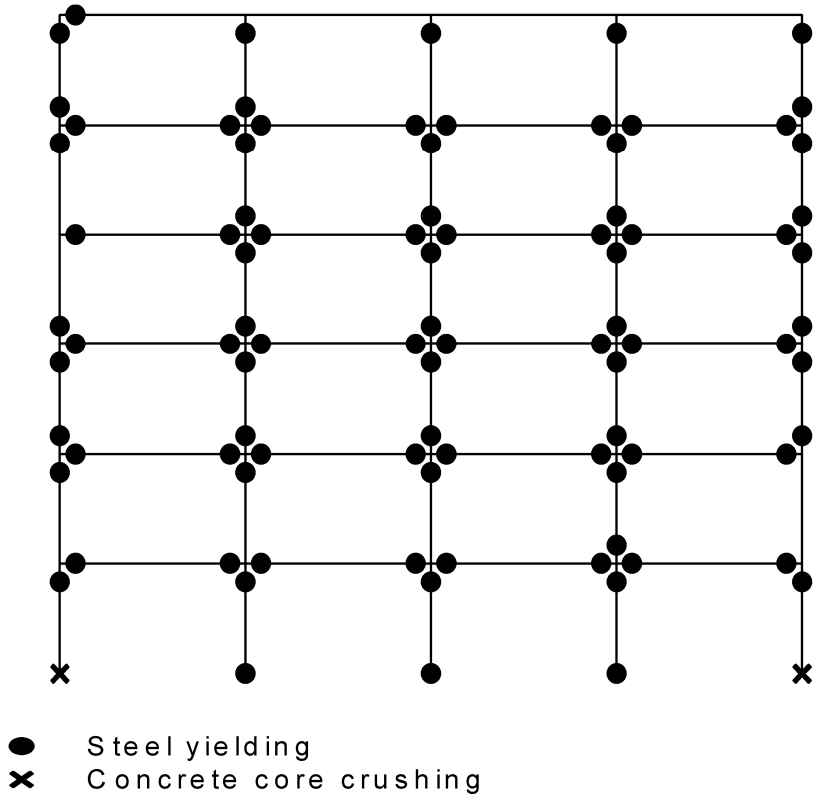
Steel yielding
Concrete core crushing

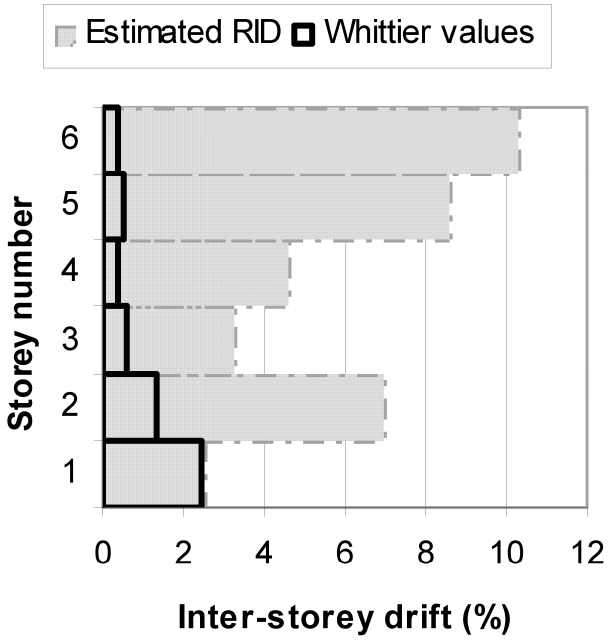


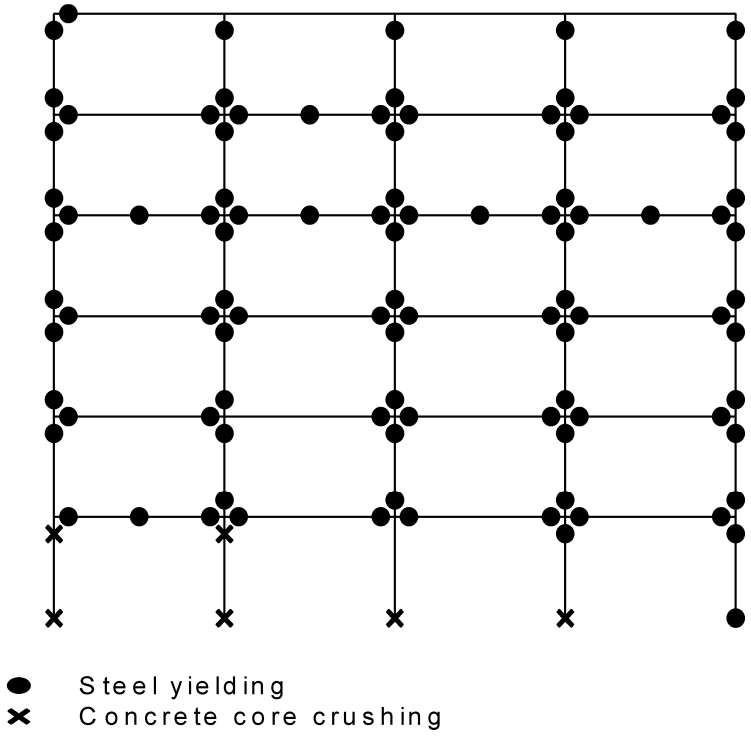


Figure 22: Results considering Whittier earthquake.

a) MIDs at Sa = 3.40g as compared to FID limits
b) Distribution of yielding and crushing at FID limit
c) RIDs at Sa = 5.00g as compared to RID limits
d) Distribution of yielding and crushing at RID limit

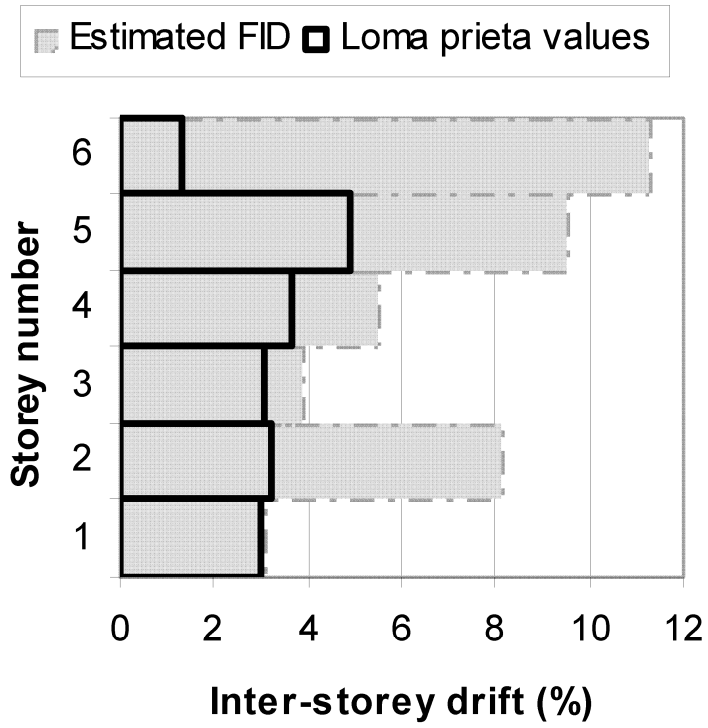
Estimated FID
Loma prieta values
Storey number
6
5
4
3
2
1
0
2
4
6
8
10
12
Inter-storey drift (%)

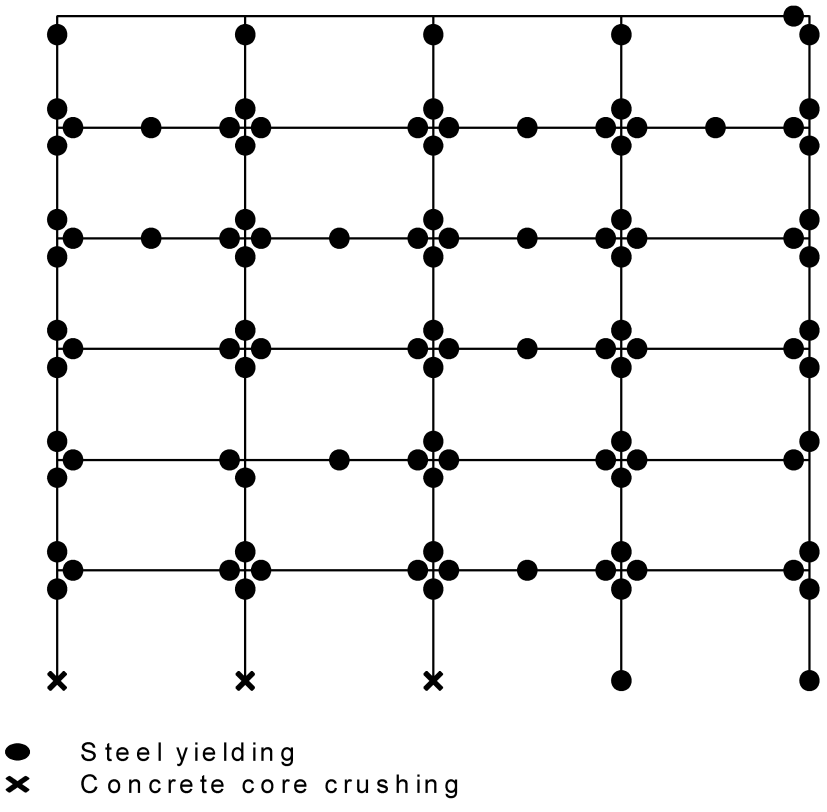
Steel yielding
Concrete core crushing

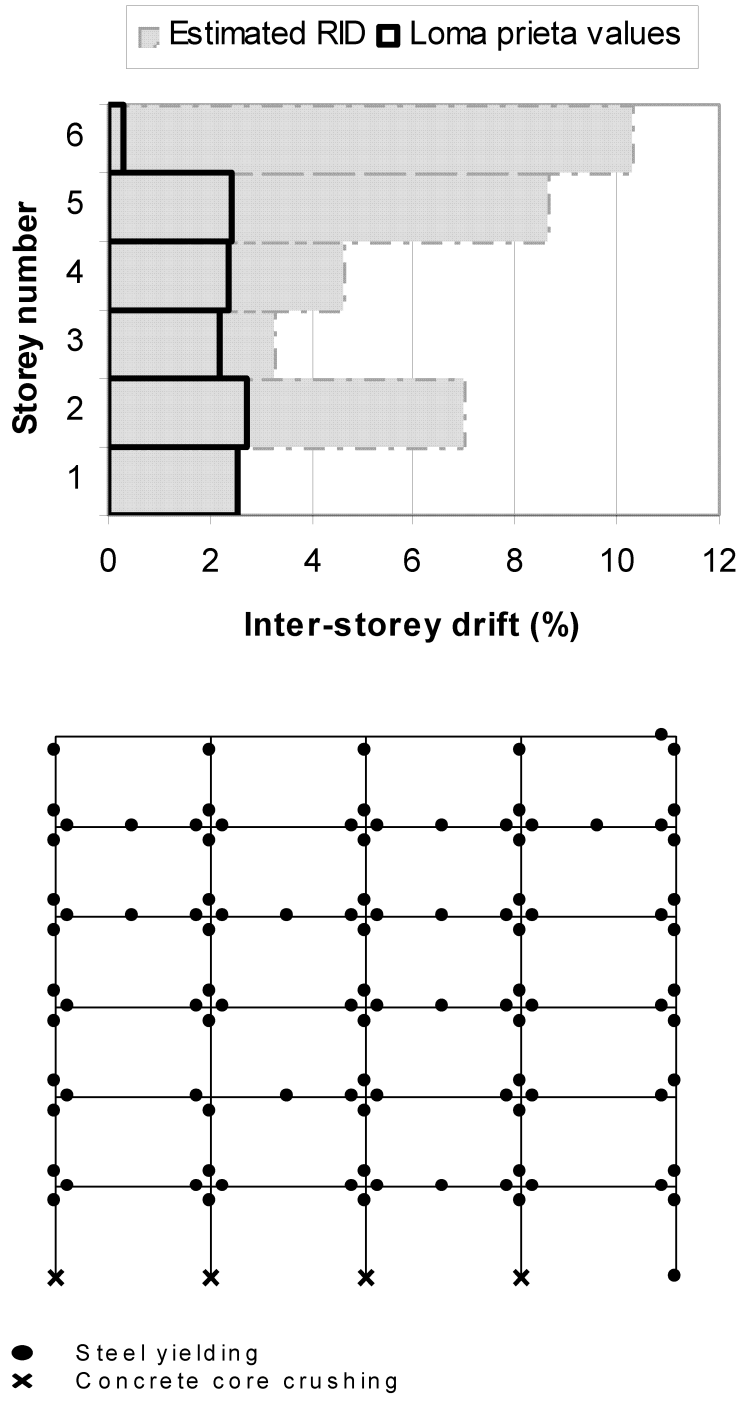


Figure 23:Results considering Loma Prieta earthquake.

a) MIDs at Sa = 4.10g as compared to FID limits
b) Distribution of yielding and crushing at FID limit
c) RIDs at Sa = 4.28g as compared to RID limits
d) Distribution of yielding and crushing at RID limit

**List of Tables:**

Table 1. Comparison between predictions of Zeus-NL and the experimental work conducted by Sakai et al. (2004)

| | 70% Scale | | | | 100% Scale | | | |
|---|---|---|---|---|---|---|---|---|
| | N-S Direction | | E-W direction | | N-S Direction | | E-W direction | |
| | Maximum | Residual | Maximum | Residual | Maximum | Residual | Maximum | Residual |
| Experimental Disp. (mm) | 146.00 | 20.00 | 100.00 | 13.00 | 310.00 | 245.00 | 180.00 | 140.00 |
| Analytical Disp. (mm) | 125.00 | 16.00 | 95.00 | 13.00 | 280.00 | 246.00 | 180.00 | 140.00 |
| Error (%) | 14.38 | 20.00 | 5.00 | 0.00 | 9.68 | 0.41 | 0.00 | 0.00 |

Table 2. Comparison between predictions of proposed method and studies by other researchers

| | Number of stories | Number of bays | MID at Collapse (%) | | Damaged floor | |
|---|---|---|---|---|---|---|
| | | | Predicted | By others | Predicted | By others |
| Ghobarah et al. (1999) Analytical (Old codes) | 3 | 3 | 2.25 | 2.25 | 1st | 1st |
| Ghobarah et al. (1999) Analytical (new codes) | 3 | 3 | 4.86 | 4.00 to 5.00 | 1st | 1st |
| Lu (2002) Experimental | 6 | 3/2* | 4.95 | 2.40 – 6.00 ** | 1st | 1st |
| Moehle et al. (2005) Experimental | 3 | 3 | 8.15 | 9.00 | 1st | 1st |
| Haselton et al. (2008) Analytical | 4 | 3 | 4.57 | 4.00 to 12.00 | 1st | 1st and 2nd *** |

* The building has two bays at the first storey and three bays at other stories.

** The building was stable at 2.4% MID and unstable at MID 6%.

*** The collapse mechanism was a contribution between first and the second floor failure.

Table 3. Inter-storey drift magnification factors for the six-storey building

| Storey Number | 1st | 2nd | 3rd | 4th | 5th | 6th |
|---|---|---|---|---|---|---|
| Magnification factor ($m_{av}$) | 1.000 | 1.934 | 1.466 | 1.543 | 1.578 | 1.578 |

Table 4. Chosen earthquake records

| **Earthquake** | **Date** | **Ms Magnitude** | **Station** | **PGA (g)** | **A/v** |
|---|---|---|---|---|---|
| Northridge USA | 17/1/94 | 6.7 | Arleta-Nordhoff | 0.340 | Inter. |
| Imperial Valley USA | 15/10/79 | 6.9 | El Centro Array #6 (E06) | 0.439 | Low |
| Loma Prieta USA | 18/10/89 | 7.1 | Capitola (CAP) | 0.530 | High |
| Whittier USA | 1/10/87 | 5.7 | Whittier Dam | 0.316 | High |
| San Fernando | 9/2/71 | 6.6 | Pacoima Dam | 1.230 | Inter. |